

RF Engineering Meets Optoelectronics

*Stavros Iezekiel, Maurizio Burla,
Jonathan Klamkin,
David Marpaung, and José Capmany*

Integrated microwave photonics (IMWP) is concerned with applying integrated photonics technology to microwave photonic systems. It is one of the most active and exciting areas of current research and development in microwave photonics (MWP), building upon the impressive foundations of integrated photonics in various systems involving material platforms such as indium phosphide (InP) and silicon nitride (Si_3N_4). The aim of this article is to explain to the wider microwave engineering community the significance of the new

field of IMWP and to describe how it may potentially be applied to improve the performance and capabilities of microwave and millimeter-wave (mmWave) systems. Just as the microwave monolithic integrated circuit (MMIC) has revolutionized active microwave circuits, IMWP is poised to open up new applications for microwave engineering that take advantage of the unique functionalities offered by photonics, especially with regard to its large bandwidth.

Working on the assumption that most microwave engineers may be somewhat unfamiliar with the

Stavros Iezekiel (s.iezekiel@ieee.org) is with the Department of Electrical and Computer Engineering, University of Cyprus, Nicosia, Cyprus. Maurizio Burla (maurizio.burla@emt.inrs.ca) is with the Institut National de la Recherche Scientifique-Énergie, Matériaux et Télécommunications, Varennes, Quebec, Canada. Jonathan Klamkin (klamkin@bu.edu) is with the Department of Electrical and Computer Engineering, Boston University, Massachusetts, United States. David Marpaung (david.marpaung@sydney.edu.au) is with the Centre for Ultrahigh Bandwidth Devices for Optical Systems, Institute of Photonics and Optical Science, School of Physics, University of Sydney, New South Wales, Australia. José Capmany (jcapmany@iteam.upv.es) is with the Instituto de Telecomunicaciones y Aplicaciones Multimedia, Ciudad Politécnica de la Innovación, Valencia, Spain.

Digital Object Identifier 10.1109/MMM.2015.2442932
Date of publication: 7 August 2015

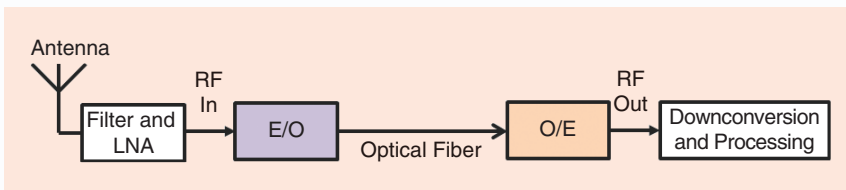


Figure 1. An analog optical fiber link as an example of an MWP system for transporting RF signals over optical fiber. In many links, the E/O module consists of a laser and optical intensity modulator, with the RF input being applied as the drive voltage to the modulator. The O/E module consists of a photodiode that recovers the microwave signal as a photocurrent. LNA: low-noise amplifier.

prospects of regular MWP technology, we begin by briefly describing the main characteristics, advantages, and uses of MWP. We then move on to describe how IMWP will enable performance improvements and new functionalities for microwave systems based on photonics. Our overview will discuss various IMWP material platforms and devices, and we will also outline how IMWP can be used in microwave systems, focusing specifically on the important example of antenna beamforming.

What Is Microwave Photonics?

MWP is an interdisciplinary field that unites the domains of RF engineering and optoelectronics [1]–[4]; an MWP system will typically contain a mix of microwave and photonic components configured such that microwave signals are transported (and, quite often, processed) in the optical part of the spectrum using a variety of photonic components, such as lasers, optical fiber, and, in the most basic systems, photodiodes. A good example of a first-generation system is an analog intensity-modulation optical link of the type shown in Figure 1, which consists of a device for converting microwaves to a microwave-modulated optical signal [electrical-to-optical (E/O) converter], a fiber over which the microwave signal propagates as the narrowband modulation of an optical carrier, and then a photodetector for conversion back to the microwave domain [optical-to-electrical (O/E) conversion].

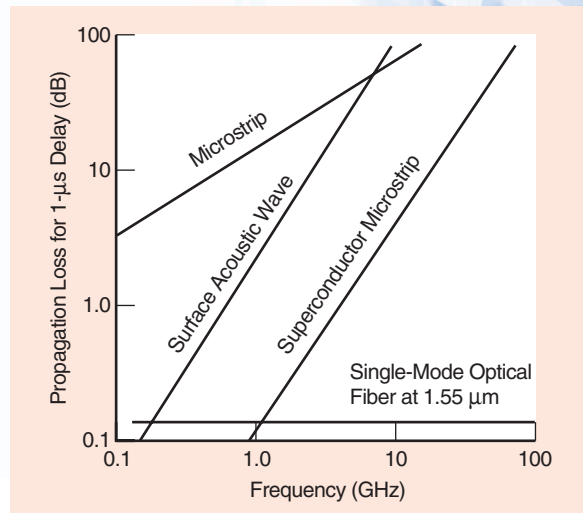


Figure 2. A comparison of the propagation loss, based on a delay of 1 μ s versus frequency, between three microwave transmission media and optical fiber. In the case of optical fiber, the frequency corresponds to that of the RF input signal (as shown in Figure 1); the effects of E/O and O/E conversion are not accounted for. (Figure adapted from [4].)

The motivation for this approach is the large bandwidth and relatively low loss per unit length of optical fiber compared with that of conventional microwave transmission media (Figure 2) in addition to its electromagnetic immunity and mechanical flexibility—all of which make the approach ideally suited to antennas

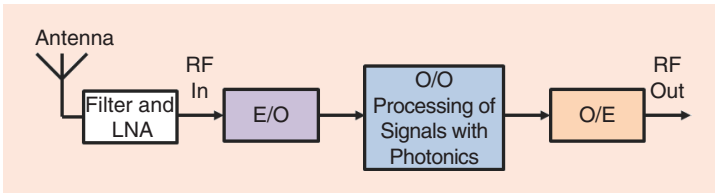


Figure 3. Analog optical processing of microwave signals. In this advanced application of MWP benefiting from photonics' broad bandwidth, not only are RF signals transported in the optical domain, but a variety of signal processing functions can also be implemented via optical input–optical output (O/O) components.

located remotely over several kilometers. It should be noted that the contributions of the E/O and O/E conversion stages are not accounted for in Figure 2, and the square-law nature of photodetection means that an optical loss of approximately 0.2 dB/km will translate into a corresponding electrical loss of 0.4 dB/km. Moreover, the presence of active devices in both the E/O and O/E stages means that, in addition to the overall link gain, it is also necessary to evaluate link performance with respect to noise figure, third-order intermodulation products, and spurious free dynamic range (SFDR). Nevertheless, over several kilometers, an analog optical fiber link can prove attractive for

the remote location of antennas, where conventional microwave cables would incur too much loss.

In the 30 years since the earliest work on analog links, the field of MWP has attracted immense interest and generated many new developments from both the research community and the commercial sector. Emerging applications for future 5G networks and subterahertz systems, including radio-over fiber (ROF), indicate that MWP is set to be a subject of increasing importance [5].

From one perspective, MWP deals with the application of microwave engineering to high-speed photonic devices—e.g., in the design of traveling-wave (TW) electrodes for optical intensity modulators or that of matching networks for analog links (such as that shown in Figure 1). In fact, the Mach-Zehnder modulator (MZM) is an early example of the integration of guided-wave photonics with TW structures that highlights the need for performance optimization through such integration.

The real significance of MWP, however, is as a disruptive technology in which the application of photonic components, systems, and techniques enhances

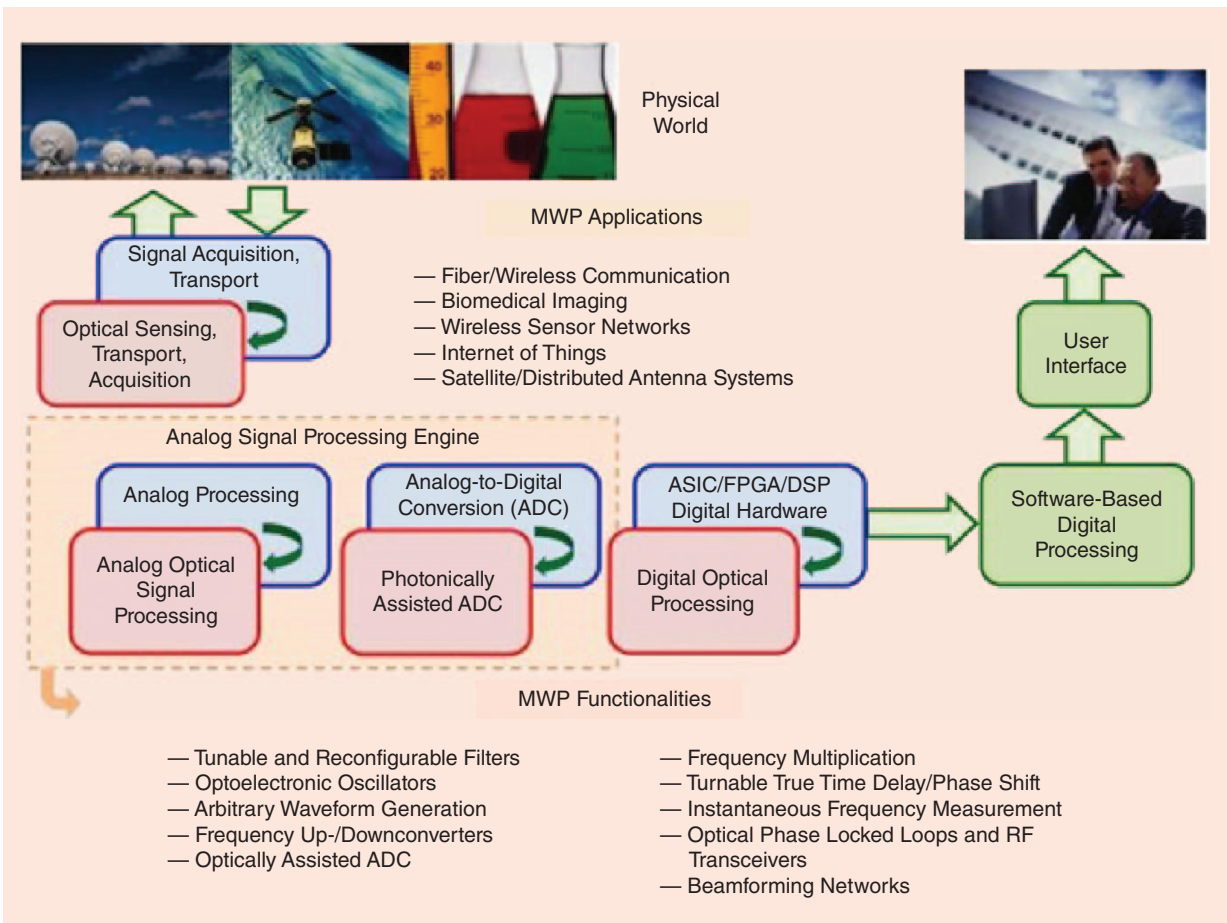


Figure 4. Conceptual rendering of an analog signal processing engine within the broad context of multiple ICT systems. ASIC: application-specific integrated circuit; FPGA: field-programmable gate array.

microwave and mmWave systems, yielding performance improvements and adding new functionalities that would not be possible using an electronic-based approach. Looked at from this perspective, it is more accurate to say that MWP deals with the generation, processing, and distribution of microwave and mmWave signals by optical means, benefiting from photonics' inherently unique advantages, such as low loss (independent of frequency), high bandwidth, and immunity to electromagnetic interference [1]–[4]. Moreover, MWP adds fundamental value by enabling key functionalities to be realized in microwave systems using photonics, as suggested in Figure 3. These include filtering, arbitrary waveform generation, frequency upconversion/downconversion, and instantaneous measurement, all of which are quite complex or, in some cases, not even possible using RF techniques alone.

In addition, MWP creates new opportunities for information and communication technology (ICT) systems and networks. While initially research activity in MWP focused on defense applications such as photonically enabled radar and remote siting of antennas via analog optical fiber links, as shown in Figure 1 [6], it has now expanded to civil scenarios, spanning conventional areas such as cellular [7], wireless [8], and satellite [9] communications, distributed antenna systems [10], and optical signal processing [11] as well as emerging fields such as converged fiber–wireless [12] and in-home networks [13], medical imaging systems using terahertz waves [14], wireless body and personal area networks [15], and instrumentation and the Internet of Things [16].

MWP systems are usually at the heart of the analog signal processing engines placed between signal acquisition devices and front-end digital signal processors (DSPs) to match the signal formats with the constraints imposed by DSP-limited sampling rates, as shown in Figure 4, which can realize a wide variety of functionalities.

Why IMWP?

Despite the tremendous potential of MWP, the technology's widespread use and application are currently limited by the high cost, bulkiness, complexity, and power consumption of its systems. The typical size, weight, and power consumption (SWAP) figures for commercial MWP systems are around 0.04–0.2 m² (size), 1.5–10 kg (weight), and 15–20 W (power consumption) [17], making them unsuitable for mass production and widespread use as required by the next-generation and emerging applications outlined here.

Therefore, the major challenge MWP researchers must overcome is reducing cost and SWAP. It is expected that solving this problem will have dramatic scientific, technical, and economic impacts in those areas where SWAP is critical (e.g., airborne systems) or where a large number of devices are needed (e.g., radio astronomy arrays); both of these applications benefit from complex optically

steered arrays, which, in turn, represent an ideal example of IMWP systems, as illustrated in Figure 5. However, there are also benefits to be had from IMWP for simpler MWP systems such as analog optical links, where IMWP devices can be used to improve dynamic range through tunable optical filtering [18] or novel link architectures requiring balanced detection [19].

Integrated photonics has the potential to change the power-scaling laws of high-bandwidth systems through proper architectural choices that combine photonics with electronics to optimize performance, power, footprint, and cost [20]. In particular, analog photonics has a qualitatively different behavior compared with digital electronics because the energy per analog task is dominated by the steady-state bias power and does not increase significantly as the bandwidth increases [20]. Furthermore, most photonic devices are currently highly temperature dependent and so require temperature regulation, which consumes the majority of bias power. As integrated photonics favors alternative means of temperature control that draw less power, the power consumed by photonic devices can be reduced drastically. IMWP [22] that aims at incorporating MWP components/subsystems in monolithic or hybrid photonic circuits is instrumental in achieving the aforementioned objectives. Research activity in IMWP has been almost exclusively focused toward application-specific photonic integrated circuits (ASPICs) where a particular circuit and chip configuration is designed to optimally perform a specific MWP functionality.

An important point to note is that IMWP may not necessarily be confined to applications involving optical fiber inputs and outputs but can be used to implement RF photonic signal processing for a front end, as shown in Figure 6. Here, there are only RF external ports, with the photonics confined to the core of the chip only. In this respect, IMWP can complement rather than fully replace MMICs to overcome their limitations in terms of bandwidth, frequency independence, and losses at mmWave and terahertz frequencies. A very early and basic example of this philosophy is the implementation of a microwave amplifier using cascade connections of lasers coupled to an array of photodiodes, all fabricated on a single chip [21].

Applications of IMWP

In the same way that MMIC technology has been used to implement a wide array of functions for microwave systems, we envisage that IMWP will be a key enabling technology in realizing compact versions of existing MWP systems in addition to emerging MWP applications. There are already examples of IMWP chips in high-dynamic-range MWP links, MWP filters, photonic generation of mmWave and terahertz signals, and instantaneous frequency measurement (IFM) and arbitrary waveform generation [22]. Here, we will focus on

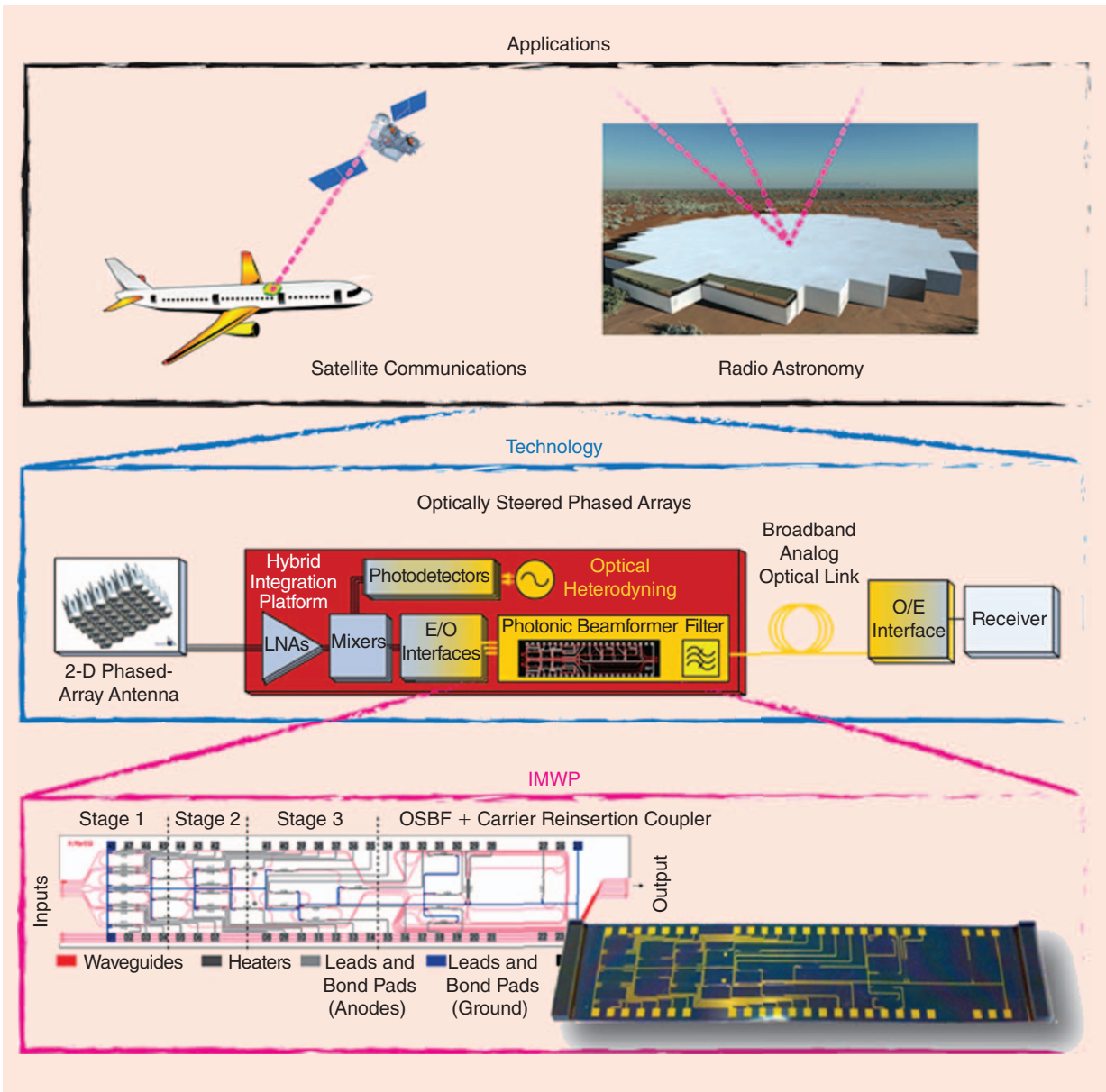


Figure 5. Typical applications of optically steered phased arrays that may be implemented with IMWP. Here, it is envisaged that an IMWP chip, as shown at the bottom, would offer high levels of integrated functionality but would be combined with microwave circuits and E/O interfaces on a hybrid platform, as shown in the middle. (Figure adapted from [36].) OSBF: optically steered beamformer.

one particular application, photonic beamforming, to illustrate the increasing level of activity in IMWP.

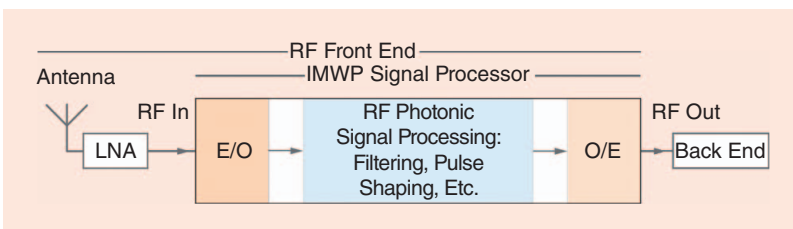


Figure 6. Conceptual rendering of an IMWP-based RF front end. The approach is similar in philosophy to that of low-frequency optocouplers, electronic devices in which the key function (in this case isolation) is performed optically, but the external terminals and ports are electrical.

Phased-array antennas offer attractive characteristics in terms of beam reconfiguration capability, electronic scanning, beam shaping, interference nulling, and robustness [23], [24]. The radiation characteristics of the array can be controlled by adjusting the complex excitations (in magnitude and phase) of the individual antenna elements. These are provided using a feeding network, or beamformer, performing the basic functions of signal splitting, and combining phase shift and/or time delay. Time delay is important for broadband applications

to provide the same beam pointing direction across frequency and avoid the phenomenon of beam squint [22]. As a consequence, the performance of the array is strongly linked to that of the variable phase shifters and delay lines employed. In particular, reconfigurable true-time-delay (TTD) lines with ultrabroadband (up to hundreds of gigahertz) and fast and continuous reconfiguration capability are required for modern phased arrays that are employed, e.g., in communications and radar systems.

Photonic Beamforming

The use of photonics techniques for antenna feeding has been regarded with interest for more than two decades [25]. IMWP signal processing techniques allow the implementation of broadband, highly flexible, and frequency-independent TTD and phase shifters. TTD allows broadband beamsteering operation, while phase shifters are used in narrow-band applications. In optical beamforming, the broadband time delay or phase shift of microwave signals is achieved in the optical domain, by providing time delay to an optical carrier signal that is modulated with the electrical signal of interest. The main driver behind the use of photonic techniques for TTD has been the very low loss and large delay achievable at microwave and mmWave frequencies by means of optical fibers [23].

Main Approaches

Optical delay lines can be classified into two main categories: variable-length delay lines (VLDL) and variable-propagation-velocity lines (VPVL) based on optical filters. Historically, VLDLs were the first to be proposed. Their simplest and most common implementation is in the form of switched delay lines (SDLs), where the amount of delay is changed in discrete steps by selectively interconnecting a cascade of optical paths of different lengths by means of optical switches. Fiber-based SDLs have been proposed with on-chip switches that offer larger delays and higher compactness with respect to bulk optics delays, while retaining very low loss due to the use of optical fibers.

Integrated switches were proposed as early as 1984 in lithium

niobate (LiNbO₃) [26], followed by gallium arsenide (GaAs) [27], and InP [28]. In this approach, the main loss contribution is related to the fiber-to-chip coupling losses. Several successful system demonstrations of squint-free radar systems have been shown employing these approaches that are capable of simultaneous X- and L-Band operation [29] and feeding a 16-element L-Band radar [30]. A review of the most significant demonstrations has been given in [31].

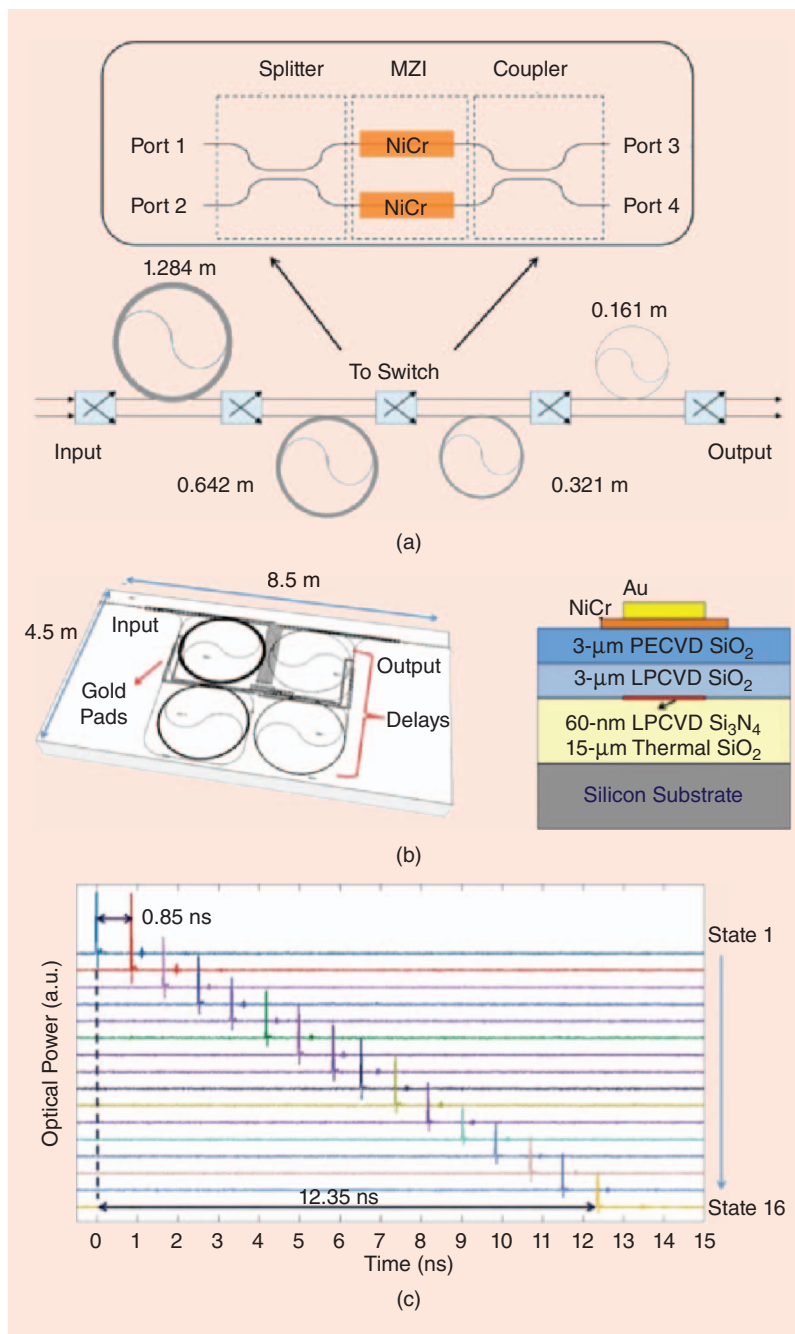


Figure 7. A 4-bit on-chip tunable delay: (a) a schematic with delay lengths in each stage, (b) the chip cross section, and (c) the demonstration of pulse delay in all settings. NiCr: nickel-chromium; PECVD: plasma-enhanced chemical vapor deposition; LPCVD: low-pressure chemical vapor deposition; SiO₂: silicon dioxide. (Figure adapted from [49].)

The requirements on total delay, resolution, and stability for photonic delay lines are highly application dependent. In general, larger antennas with wide scanning range require larger delays and provide narrower fractional bandwidths [32] if based on phase shifters only. Examples reported in the literature have shown that for radar applications in the 3–6-GHz band, group delays with continuous tuning up to 30 ns are needed and can be achieved by means of optical techniques, with a 6-bit resolution [33]. Subpicosecond delay resolution and stability are needed when operating in mmWave ranges and can be achieved, e.g., using fiber stretchers [34] or on-chip delay lines [35]. Further examples of requirements for applications to satellite communications and radio astronomy have been discussed in [36].

More recently, optical SDLs have been proposed in a completely integrated photonics form (including the delay lines), allowing increased compactness and improved stability versus thermal and mechanical stress, with reduced delay switching times reaching a few tens of nanoseconds [29]. Higher delay resolution (required for antennas operating at high frequency) can also be improved with an integrated photonics approach. A number of photonic integration platforms have been used, such as polymer technology [37]–[39], silica [40]–[43], LiNbO₃ [44], GaAs [45], [46], and InP [47], [48]. A recent example [49] using ultralow-loss Si₃N₄

substrate showed a fully integrated 4-bit TTD line capable of delays above 12 ns, corresponding to about 2.4 m of propagation length, on a chip area of 4.5 cm × 8.5 cm, with waveguide losses as low as 1 dB/m (Figure 7).

Optical filters or dispersive optical transmission lines are also employed to implement tunable delay lines. Due to chromatic dispersion in optical fibers (which results in group velocity dispersion [50]), carriers at different wavelengths experience different group delays. Therefore, different RF delays can be achieved by simply adjusting the wavelength of the optical carrier, which is modulated with the electrical signal to be delayed. One advantage of VPVL techniques is the continuous delay tuning capability that translates into the possibility of continuous steering of the antenna beam direction.

An example of a VPVL is the well-known fiber-optic prism, first proposed by Esman [51], where dispersive fibers with different lengths provide different delays to the individual antenna elements of the array. Using this method, squint-free multioctave beamsteering over ±53° and a 2–18-GHz bandwidth has been shown for an eight-element transmit array [52]–[55]. An evolution of this scheme is represented by the programmable dispersion matrix, where a single dispersive fiber is employed; signals feeding the different antenna elements are modulated onto different wavelengths and multiplexed on the fiber using a multiplexer and demultiplexer. This technique reduces the bulk, requiring a single delay line for the complete array, while at the same time improving the delay stability and demonstrating ±60° steering capability over K_a-Band.

Fiber Bragg gratings have also been proposed to replace dispersive fibers [56], [57], and on-chip chirped gratings have been recently demonstrated by Giuntoni et al. [58] in SOI technology, capable of variable delay up to 450 ps.

A different approach for wavelength-selective routing of signals through delay lines of different length is based on arrayed waveguide gratings (AWGs) [59]. These are multiport devices that allow one to selectively route the power from the input to a specific output, based on its frequency. By connecting lines of different lengths to the ports, as represented in Figure 8, it is again possible to select the desired delay line by varying the carrier wavelength. Yegnanarayanan et al. [60] demonstrated a wavelength selective time delay based on a recirculating AWG. An 8-bit TTD employing silica waveguide delay lines was shown, operating in C-Band (1,550 nm) and with a 0.8-nm channel spacing. Recent demonstrations have been proposed in silicon on insulator (SOI) for application to indoor 60-GHz communications [61]. The main issue in this scheme is the temperature fluctuation of the spectral response of the AWG, with a drift of approximately 1 GHz/°C, which can be compensated using active temperature stabilization.

A similar example of a fully integrated beamformer in InP technology was proposed in [29]. Four separate

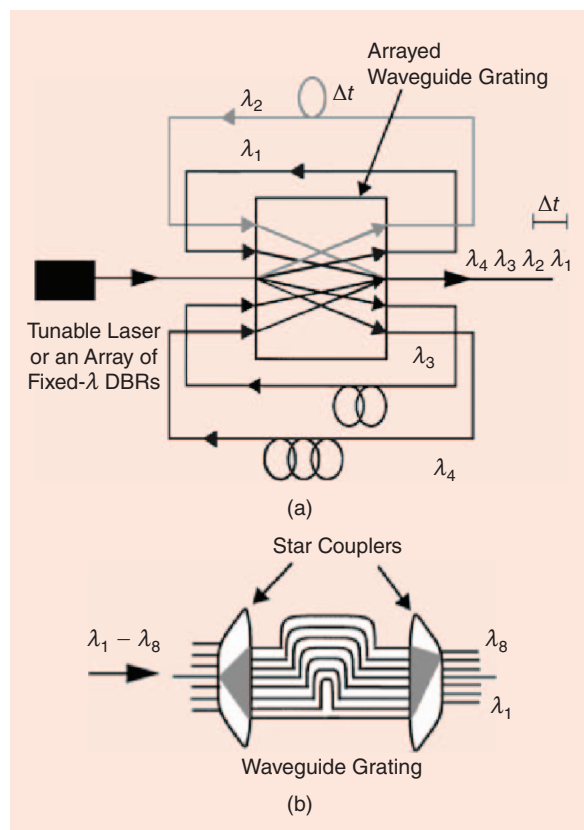


Figure 8. (a) An AWG-based tunable delay line. (b) The schematic of an AWG demultiplexer. (Figure adapted from [60].) DBR: distributed Bragg reflector.

wavelengths generated by four different lasers are multiplexed and then inserted on the chip, where an AWG is used to demultiplex and route them to four different delay lines with 3 bits each. The number of bits is limited by the size of the InP wafer. A different version was proposed where only the AWG is implemented on chip, and the delays are based on optical fibers, allowing a larger number of bits and delays but also leading to undesirably high fiber-to-chip coupling losses. In addition, bidimensional beamformers have been developed, where separate cascaded stages are used for azimuth and elevation control [62]. Vidal et al. [63] proposed an interesting solution where AWGs are combined with highly dispersive fibers to realize a multibeam architecture, exploiting the frequency periodicity of the AWG.

Recent Developments

Recent development efforts have been directed toward on-chip implementations of optical delay lines for improved compactness, low cost, higher phase stability and robustness to environmental fluctuations, and faster switching speeds. Photonic crystals have been employed as a single fully integrated dispersive delay element. Sancho et al. [64] demonstrated the use of a single, very compact, low-loss photonic crystal to implement multiple variable TTDs, as shown in Figure 9. The operation is based on the slow-light properties of photonic crystals, in which the group delay can be increased to very high values depending on the wavelength. The authors demonstrated a 1.5-mm-long device capable of generating delays up to 70 ps with losses below 10 dB over the complete 0–50-GHz band.

Integrated optical filters have also been used to implement broadband tunable optical delays. Cascaded optical ring resonators (ORRs) have been demonstrated in silica [40], [43], TriPleX [65], and SOI [66], [67]. A complete beamformer based on ORRs arranged in a binary-tree network architecture was demonstrated in [68]–[73], with [73] fabricated in

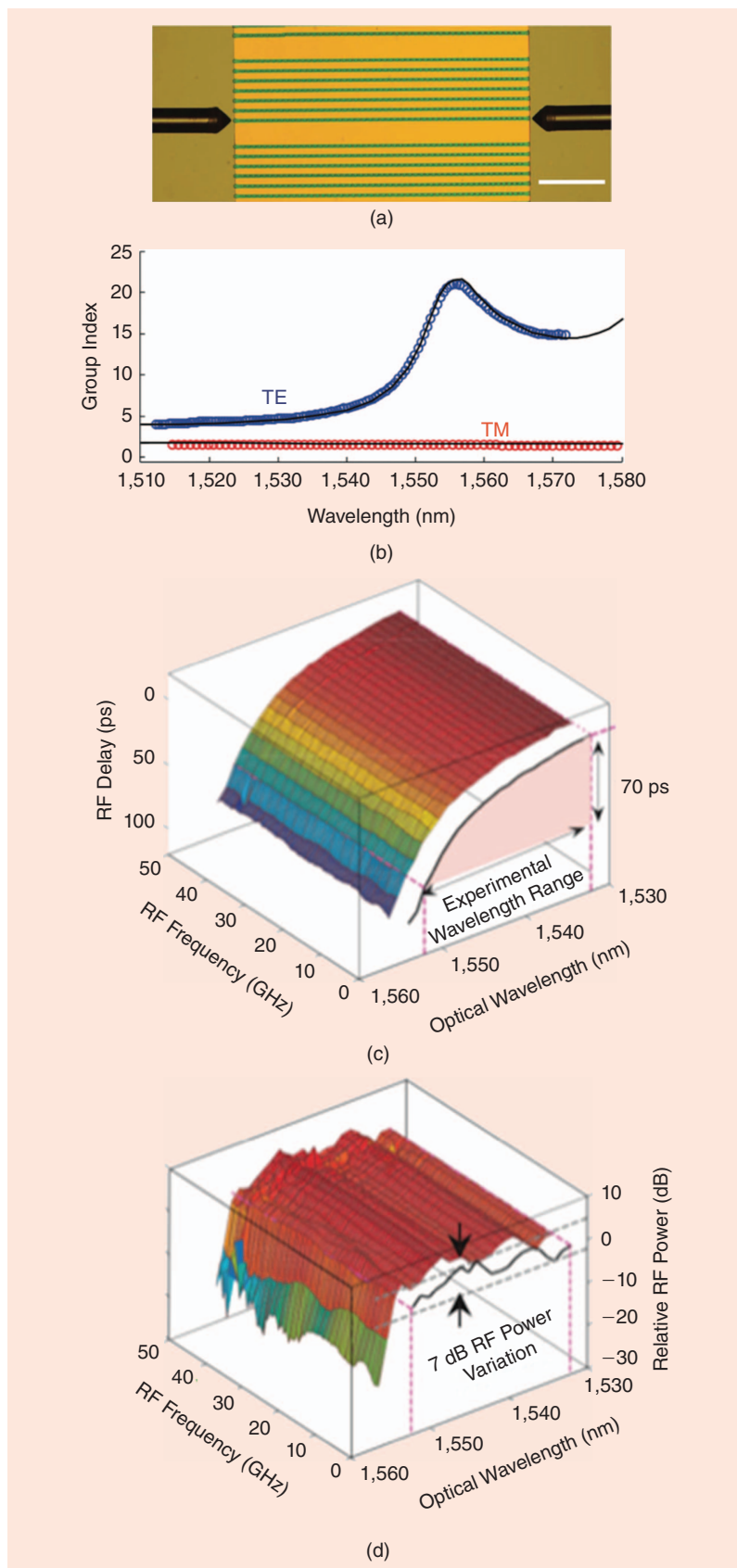


Figure 9. (a) A photonic crystal waveguide employed as a tunable delay line. (b) Group index versus wavelength for transverse electric (TE) and transverse magnetic (TM) modes. (c) Delay and (d) power fluctuation of the microwave signal as a function of carrier wavelength. (Figure adapted from [64].)

TriPleX waveguide technology. Delays up to 1.2 ns were shown over a bandwidth of 2.5 GHz for K_u -Band satellite communication applications [71], [72], [74] and radio astronomy [75], for which a system demonstration of squint-free beamsteering of a four-element array was shown. More advanced hardware compressive architectures featuring multiwavelength operation and exploiting the frequency periodicity of ORR filters have recently been reported [75], with instantaneous bandwidths in excess of 8 GHz. In [36], a processor including an optical sideband filter, a 360° phase shifter, and a TTD unit providing delays up to 400 ps has been demonstrated on a single chip.

In some applications, it is sufficient to provide narrowband phase shift to the antenna elements. Optical techniques are of interest, as they have shown the ability to create constant phase shift over ultrabroad bandwidths of tens or hundreds of gigahertz. Early examples have been shown in LiNbO_3 [41] and InP [44], where a 16×1 beamformer allowing amplitude and phase control was implemented in a chip of $8.5 \text{ mm} \times 8 \text{ mm}$. Beamforming up to 60-GHz carrier frequencies has been demonstrated with a similar technique [76].

Waveguide Bragg gratings realized on SOI have shown the ability to implement tunable time delays as well as ultrabroadband phase shifts in conjunction with optical single-sideband modulation. In [76], a very compact device (only $130\text{-}\mu\text{m}$ long) was employed to create broadband phase shifts for RF frequencies beyond 900 GHz. Nonlinear optics effects have also been recently employed for IMWP [78], [79]. Pagani et al. [80] have shown a phase shifter based on stimulated Brillouin scattering (SBS) providing a full 360° phase shift over a 40-GHz bandwidth with a phase-dependent insertion loss variation of only 0.5 dB. Polarization control has also been employed as an additional degree of freedom in the control of the amount of delay [81].

Besides large bandwidth, fast reconfiguration with times scales on the order of nanoseconds or less is needed, e.g., in modern radar applications or ultrawideband RF pulse generation and processing. Bonjour et al. [82] proposed a novel delay architecture named complementary phase-shifted spectra that promises tens of picosecond switching speeds. Nanosecond-time switching among different delays has already been shown in integrated

form by Wang et al. [83] for application to arbitrary waveform generation.

Current efforts aim at integrating tunable optical delays and phase shifters with active functions, i.e., modulation and photodetection, in a single package. Both monolithic realization and hybrid integration approaches are being considered, as we will discuss in the following section.

Integration Technologies and Platforms

Overview

A number of integration technologies and platforms are available for IMWP, including monolithic, heterogeneous, and hybrid approaches. Monolithic implies a single material system or a single-chip implementation. Heterogeneous approaches integrate more than one material system into a common process, an integration that can be accomplished by initially synthesizing materials on foreign substrates or bonding different materials together. Hybrid integration generally implies that separate chips are brought together in backend steps such as die-attach or flip-chip bonding to produce multichip modules (MCMs).

A widely-known example of a photonic MCM is silicon optical bench technology, which supports the passive alignment of optical fibers to devices such as laser diodes that can be flip-chip bonded to the platform [84]. Other MCM materials include composite glass–silicon wafers [85] and a polymer optical bench [86]; this latter material is useful because it supports bulk optical components such as those used in optical isolators. Although packaging is a very important aspect, much of the current research effort in IMWP is based on monolithic and heterogeneous approaches.

Typical components used in IMWP include lasers, modulators, photodetectors, optical amplifiers, optical switches, and optical filters, along with passive components, such as couplers, splitters, and delay lines. Several integration platforms exist for realizing IMWP systems, and the characteristics of the integrated components vary widely according to the platform. The following will describe and compare integration platforms and also consider devices and device performances as applicable to IMWP. For example, for modulators, efficiency and bandwidth are critical; for lasers, narrow linewidth and low relatively intensity noise are important; for photodetectors, high responsivity and linearity are desirable.

Figure 10 shows four common photonic platforms used for IMWP: InP, silicon photonics (SiPh), planar light-wave circuits (PLCs) based on Si_3N_4 , and LiNbO_3 . Comparing and contrasting these platforms is not easy because they vary in material characteristics and device properties: meaningful

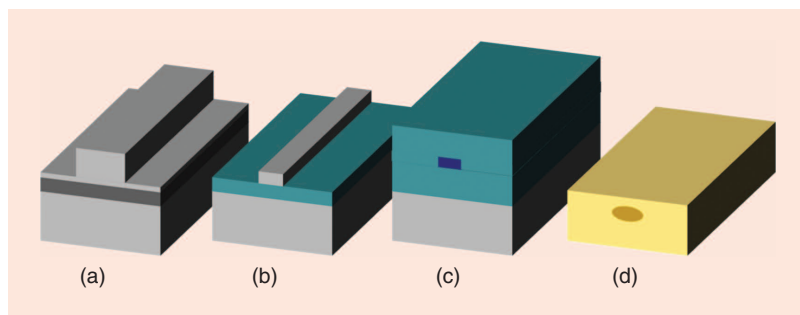


Figure 10. Waveguide structures in (a) InP, (b) SiPh, (c) PLC, and (d) LiNbO_3 .

TABLE 1. A comparison of key IMWP platforms.

Material	Advantages	Disadvantages
InP	<ul style="list-style-type: none"> • High-speed lasers, modulators, photodiodes and optical amplifiers are possible • Offers a path to integration with high-speed electronics • Has high levels of monolithic integration and good reliability 	<ul style="list-style-type: none"> • Industrial base not as well developed as for silicon CMOS processes; InP wafers are relatively small and expensive • Low index contrast makes it difficult to achieve compact passive optical components • Has high optical propagation loss
SiPh	<ul style="list-style-type: none"> • Leverages existing CMOS process technology and so is cost-effective—cheap • High index contrast allows for compact footprint for key components like ring resonators 	<ul style="list-style-type: none"> • Exhibits weak electro-optic effect • Indirect bandgap so laser integration remains difficult • Relatively high optical propagation losses; sidewall roughness must be controlled tightly to prevent scattering loss
Si ₃ N ₄ PLC	<ul style="list-style-type: none"> • Very low propagation loss makes long delays and cascades feasible, lending the platform to applications such as filtering and beamforming • Allows low-loss coupling to fiber • Cost is potentially low 	<ul style="list-style-type: none"> • Active optical devices (e.g., lasers and photodiodes) are not possible • Some complex chips (containing many ring resonators) require tuning elements and thermal control
LiNbO ₃	<ul style="list-style-type: none"> • Strong electro-optic effect and a relatively low loss make it very well suited for high-bandwidth modulators • Has a well-established technology base 	<ul style="list-style-type: none"> • Difficult to integrate with driver electronics • Requires long form factor for modulators due to interaction length between drive electrodes and waveguide • Lasing, optical amplification, and photodetection are not possible

comparisons of important features such as ease of chip-to-fiber coupling, ability to integrate various different device types and functions, and cost of fabrication are particularly challenging. However, it is possible to make some important general observations with regard to various advantages and disadvantages, as outlined in Table 1. InP, SiPh, and PLC platforms will be discussed in detail, with LiNbO₃ mentioned only briefly. [While, at present, LiNbO₃ is the preferred material for discrete MZMs and phase modulators since it offers the best combination of parameters such as power handling, optical loss, thermal stability, and efficient electro-optic conversion, it is not compatible for integration with other devices (electronic or photonic): one challenge in advancing the field of IMWP is to produce modulators that rival the performance of LiNbO₃.]

One important metric for comparing different IMWP platforms is index contrast, which, in part, governs device size and performance. Defining the index contrast as $\Delta = (n_{\text{core}}^2 - n_{\text{cladding}}^2) / 2n_{\text{core}}^2$, Table 2 summarizes the ranges of index contrast for the different platforms, along with two other important figures of merit: typical bending radius and attenuation.

The index contrast is directly related to the optical confinement of the guided modes. The higher the index contrast, the higher the confinement and the smaller the mode size. Higher confinement leads to smaller lateral waveguide dimensions but does not always lead to smaller devices because device size also includes the longitudinal dimension (i.e., the length of the device).

SiPh waveguides, e.g., can be made very small, leading to tight bend radii, which is important, e.g., in producing compact ring resonators. Some SiPh devices including MZMs, however, require long interaction lengths. InP can realize small devices and a number of active elements including lasers, modulators, and photodiodes as well as passive elements. SiPh can also realize modulators and photodetectors, but laser integration is a challenge. PLC technology is used primarily for passive components, and LiNbO₃ for modulators.

Indium Phosphide

Perhaps the most mature material system for IMWP is InP, which is a direct bandgap III-V semiconductor. InP and related materials can be grown epitaxially using techniques such as metal-organic chemical vapor deposition and molecular beam epitaxy. These techniques allow for the deposition of thin films with precise thickness and composition. Ternary compounds, such

TABLE 2. Index contrast, bend radius, and attenuation for common photonic platforms.

Platform	InP	SiPh	PLC	LiNbO ₃
Index contrast	5–10%	40–45%	0.5–20%	0.5–1%
Bend radius (mm)	0.1	0.02	0.05	0.2
Attenuation (dB/cm)	2.5	<2	0.01	0.2

as indium gallium arsenide (InGaAs), and quaternary compounds, such as indium gallium arsenide phosphide (InGaAsP) or indium gallium aluminum arsenide (InGaAlAs), can be grown on InP substrates with little or no strain. The ability to grow these and other related compounds that have direct bandgaps different from that of InP allows for multiquantum well structures that are particularly useful for realizing semiconductor diode lasers. On InP, lasers emitting in the range of approximately 1.2–1.6 μm can be realized. This wavelength range includes the common 1.31- and 1.55- μm bands used in telecommunications and MWP.

In addition to lasers, high-performance optical modulators have been realized in InP. A number of modulation mechanisms are available with InP and related materials, including the linear electro-optic effect, the Franz-Keldysh effect, the plasma dispersion effect, and the quantum-confined Stark effect (QCSE). Therefore, it is possible to engineer InP modulators for either electrorefraction or electroabsorption. An InP TW MZM was demonstrated, in [87] with a bandwidth of 63 GHz. To realize high speed and high efficiency, this modulator leveraged the QCSE and a series push-pull configuration. The device also incorporated spot size converters (SSCs) for low coupling loss to optical fiber. In [88], an electrorefractive InP TW MZM was demonstrated, employing substrate removal to realize high speed and high efficiency. This device exhibited a bandwidth of 35 GHz and half-wave voltage (V_p) of 0.8 V. Several other novel modulator structures were realized in InP, including examples with integrated lasers [89]–[91].

Regarding photodetectors, a number of structures have been developed in InP, including PIN photodiodes (PIN PDs) and unitraveling-carrier PDs (UTC PDs). PIN PDs

have been demonstrated with a 40-GHz bandwidth in an InP generic photonic integration technology [92]. UTC PDs are attractive for high-speed and high-power performance due to the elimination of holes as active carriers [92], [94]. In [95], a novel waveguide configuration with a saturation current greater than 100 mA was demonstrated.

Several InP-based integration platforms have been developed, including selective area growth, butt-joint growth, asymmetric twin waveguide, offset quantum well, dual quantum well, and quantum-well intermixing. These platforms can control the material properties selectively across the InP wafer, realizing more than one device region. A novel InP coherent integrated photoreceiver for high-linearity MWP links was realized in [96]. This receiver integrated phase modulators, UTC PDs, and passive components, including a multimode interference coupler. Examples of InP coherent photoreceivers are shown in Figure 11.

The generic InP integration platforms developed through a number of European projects have been used to realize advanced InP PICs [98]. For IMWP, several technologies were realized using this platform (more details about particular performance metrics are given in [22], [98], and [99]), including optical beamforming, fully programmable MWP filters using ring resonator structures, frequency discriminators, IFM, transmitters for terahertz applications, dual-wavelength lasers for terahertz generation, pulse shapers, arbitrary waveform generators, and monolithic-integrated optical phase-locked loops for coherent detection schemes.

Silicon Photonics

SiPh has emerged as an integration platform in recent years due to the potential for low-cost and high-volume

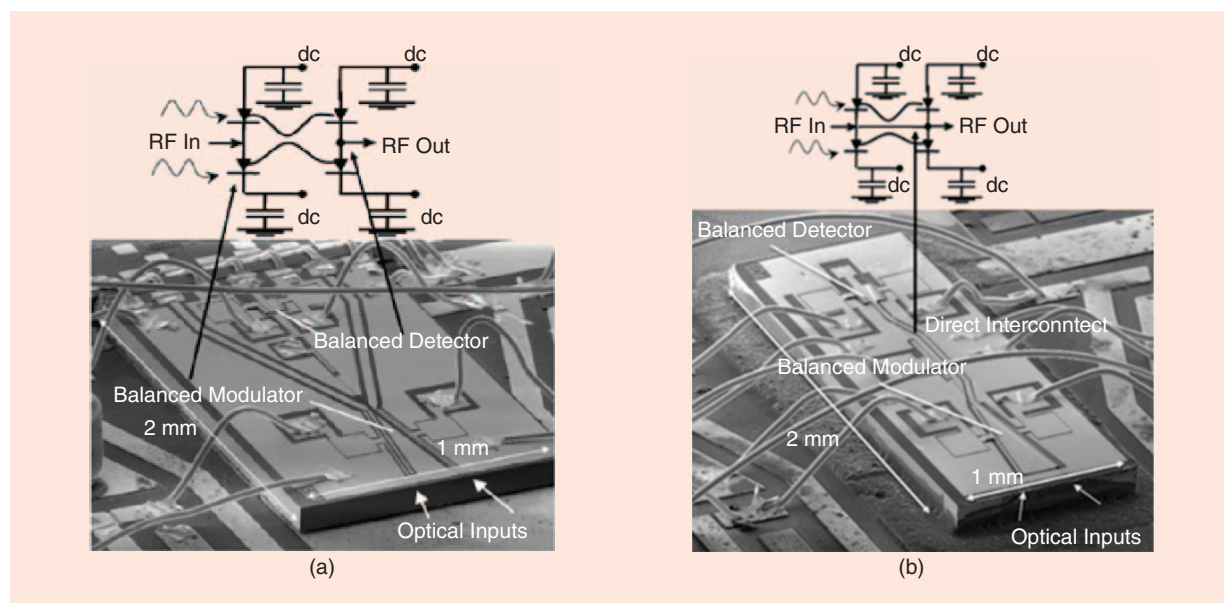


Figure 11. Images and circuit schematics of InP coherent integrated receivers: (a) an SEM image and block diagram of an integrated optoelectronic receiver [the wire bonds in the upper part connect to an integrated electronic IC (not shown)] and (b) an SEM image and block diagram of an integrated all-photonics receiver. (Figure adapted from [96].)

production. SiPh leverages CMOS processes, which are extremely mature. Unfortunately, silicon is an indirect band-gap semiconductor, and, therefore, realizing integrated lasers is a challenge. The most successful approaches to realizing lasers on silicon are based on hybrid or heterogeneous integration of III-V materials [100]. Silicon modulators, which rely on the plasma dispersion effect, are not particularly efficient. A typical $V_p L$ figure of merit for silicon MZMs is 1 V-cm [101]. For ring modulators, an extinction ratio of >5 dB has been reported with 1-V peak-to-peak drive voltage [102]. Although not particularly attractive for MWP applications due to their wavelength sensitivity, low efficiency, and low-power handling performance, the linearity of ring modulators was reported in [103]. As demonstrated, for low-dynamic-range applications, silicon ring modulators offer a compact solution.

Germanium PIN photodiodes have been demonstrated on silicon with a high 3-dB bandwidth, high responsivity, and fairly low dark current [104]. In [105], on a nonstandard SOI platform, high-power germanium photodiodes were realized and characterized for MWP applications. These photodiodes generated 14.17 dBm at 60 mA of photocurrent and at a frequency of 1 GHz.

Although the power-handling of silicon nanowire waveguides is limited, SiPh is attractive for IMWP, especially for realizing tunable optical filters [106]. In [107], a microwave photonic filter was realized with a hybrid silicon platform, as shown in Figure 12. This structure integrated thermal modulators and semiconductor optical amplifiers as control elements.

An alternative to conventional submicrometer SiPh (which has limited power handling capability) is the micrometer-scale SOI platform reported in [108], as shown in Figure 13. This platform utilizes silicon rib waveguides that are typically 4–9- μm thick. These waveguides can support higher power levels and enable better mode matching to optical fibers and hybrid-integrated components, while still utilizing CMOS processes.

In fact, most SiPh integrated circuits for MWP have been demonstrated using lower-loss rib waveguides because MWP systems entail strict requirements regarding losses to reach suitable values of dynamic range and purely passive platforms cannot make use of optical amplification. In particular, monolithic configurations have been reported (more details about particular performance metrics are given in [22] and [109]) for arbitrary

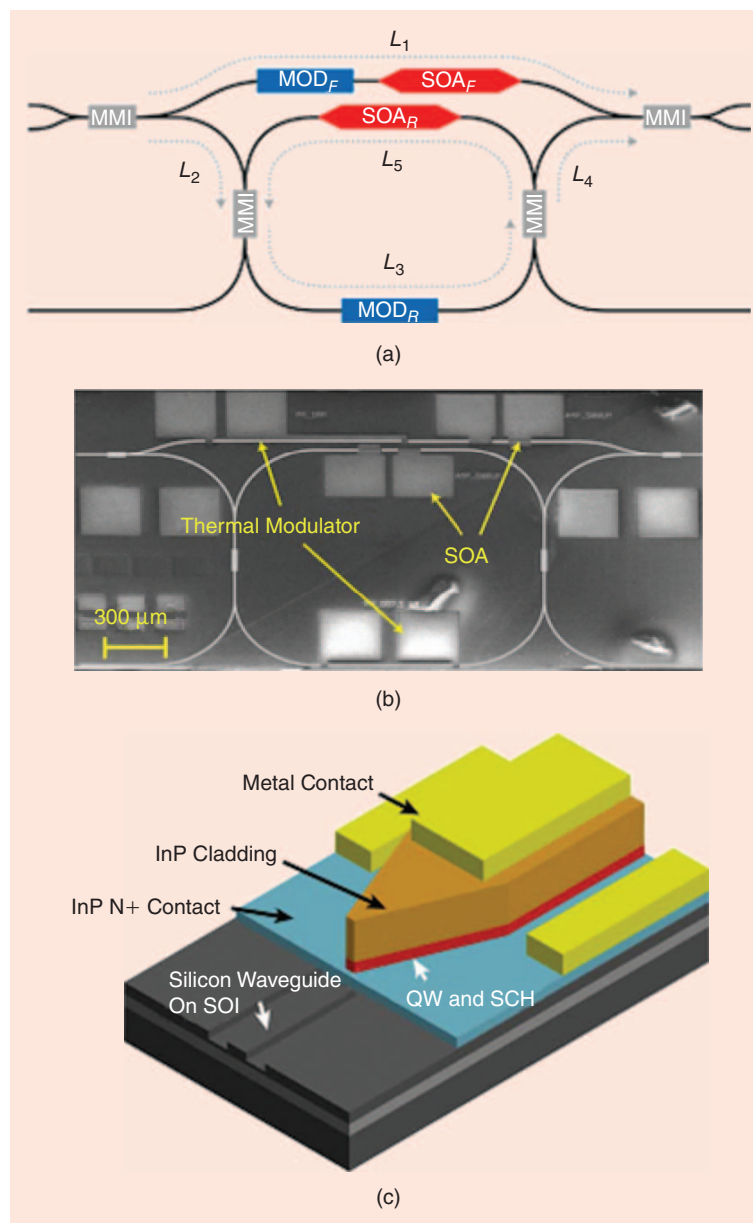


Figure 12. A hybrid tunable filter as demonstrated in [107]: (a) schematic, (b) a photomicrograph of the fabricated device, and (c) three-dimensional detail of its structure. (Figure adapted from [107].) MMI: multimode interference coupler; QW: quantum well; SCH: separate confinement heterostructure.

waveform generators, TTD lines, and beamforming networks with multigigahertz bandwidth, bandpass and notch reconfigurable filters based on Mach-Zehnder interferometer (MZI) tunable couplers, ORRs fabricated in silicon-buried channel waveguides, and, very recently, tunable phase shifters and TTD lines based on etched SOI gratings. Monolithic SOI ASPICs based on stripe waveguides have been reported for optical delay lines, arbitrary waveform generation, and ultrawideband (UWB) signal generation. Hybrid InP–silicon ASPICs have been reported for beamsteering reconfigurable bandpass filtering using ORR-loaded MZIs and, very recently, for tunable phase shifters based on disk resonators [22].

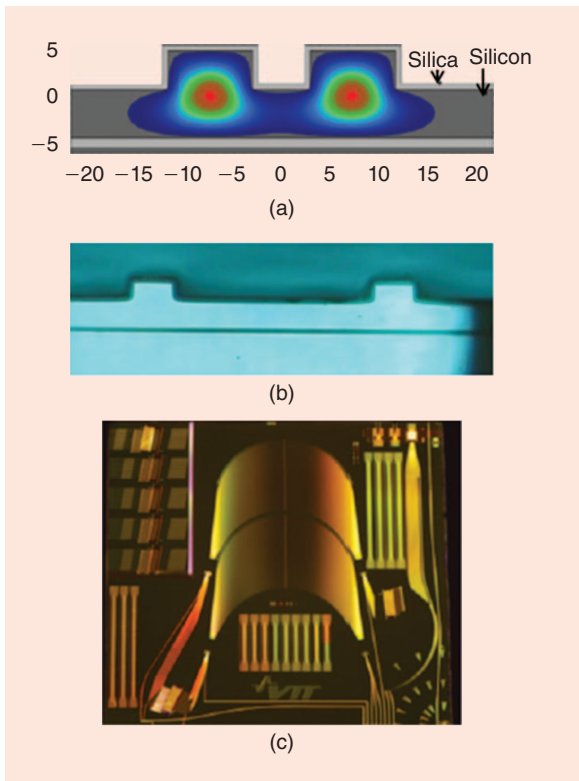


Figure 13. (a) and (b) show two micrometer-scale silicon waveguide structures, while (c) depicts a PIC demonstrated with this technology as reported in [108]. (Figure adapted from [108].)

Si_3N_4 Planar Lightwave Circuits

PLCs based on the Si_3N_4 system have low bending radii and very low propagation losses, which are of fundamental importance in the realization of IMWP signal processors. In fact, waveguides with high index contrast are desired to allow tight waveguide bends for high-density integration and a small footprint. At the same time, low attenuation is required to cascade multiple structures and implement complex processing functions on a single chip [110]. However, a tradeoff exists since high-index-contrast waveguides generally suffer high waveguide losses, mainly due to the detrimental effect of interface roughness [111].

$\text{Si}_3\text{N}_4/\text{SiO}_2$ TriPleX waveguide technology proposed by LioniX BV [112] optimizes this tradeoff, allowing high-index-contrast waveguides (20–30%) with small bending radii while keeping a very low channel attenuation (<0.1 dB/cm) [113]. This is achieved by a careful choice of the waveguide materials and of the fabrication process [102]. The waveguides are formed by growing alternating layers of stoichiometric Si_3N_4 and SiO_2 , fabricated with a low-pressure chemical vapor deposition (LPCVD) process [114]. Si_3N_4 is an attractive material because it offers a high refractive index (1.99 at 1550 nm) and a wide spectral transparency window, from far infrared to visible (wavelengths from <500 nm to >2 μm) [114]. The LPCVD technique allows accurate thickness control down to the

nanometer scale, with limited surface roughness, resulting in very low propagation losses [115]; in addition, it is a CMOS-compatible fabrication process, allowing low cost for large-volume production. Details on the fabrication steps are described in [115] and [116].

Birefringence and minimum bending radius can be controlled by design by adjusting the cross-sectional geometry [111]. TriPleX is commonly produced in three different waveguide geometries: 1) box-shaped (cross-sectional dimensions ≈ 1 $\mu\text{m} \times 1$ μm), with minimum birefringence ($\ll 10^{-3}$), losses on the order of 0.6–1.2 dB/cm, and bending radii of approximately 150 μm ; 2) double-stripe (1 $\mu\text{m} \times 1$ μm), with an average waveguide loss of 0.095 dB/cm for a bend radii ≥ 70 μm [36]; and 3) single-stripe (with a core thickness of 40 nm and a width of 13 μm) that allows ultralow losses as low as 0.45 dB/m (current world record) [113] and high birefringence.

Its record low loss makes this technology particularly suitable for implementing long delay lines useful for IMWP applications such as beamforming [49], filtering [114], and arbitrary waveform generation [115]. Based on a limited number of fundamental building blocks, i.e., optical waveguides, phase shifters, and directional couplers, complex tunable filters have already been fabricated and demonstrated, such as MZIs, ring resonators with add and drop ports, and more complex optical filters based on a combination of those with flattened passband and sharp transition bands [36], [115]. Complex microwave photonic signal processors have been demonstrated with this technology, i.e., optical beamformers [72] and high-selectivity microwave photonic filters [116]. An example of a 16×1 beamformer chip is shown in Figure 14 and illustrates well the level of complexity that is possible through the use of several cascaded ring resonator elements [117], [118].

This technology has the drawback that no active components can be realized (optical sources, modulators, detectors, or amplifiers). Active functions are added by hybrid integration to active materials such as InP and SOI [96]. SSCs for chip-to-chip and fiber-to-chip coupling have been implemented in TriPleX, with measured chip-to-chip coupling losses as low as 2.2 dB [115].

Chalcogenide

Chalcogenide glass (ChG) is the class of amorphous semiconductors that contains as a major constituent one or more of the chalcogen elements from group 6A of the periodic table (sulphur, selenium, and tellurium, but excluding oxygen), covalently bonded to other elements such as arsenic, germanium, antimony, gallium, silicon, or phosphorus [119]. ChGs offer striking properties such as a high refractive index of 2–3, transparency up to the midinfrared wavelengths, and a high nonlinear refractive index n^2 up to a thousand times that of silica. In addition, ChGs are free from nonlinear losses such as two-photon absorption [120]. A typically reported ChG optical waveguide consists of an arsenic trisulfide (As_2S_3) core on

silica, with silica or polymer overlaid [Figure 14(a)]. The most common waveguide geometry is a rib waveguide with a cross section of 2–4 μm by 0.85 μm [111].

Most of the developments of ChG waveguides have been directed toward ultrafast optical signal processing for high-speed optical communications [112]. However, the recent paradigm shift in IMWP where nonlinear optical processes are harnessed for enhanced RF signal processing has seen applications of ChG waveguides for MWP. Tan et al. [121] implemented cross-phase modulation in a 7-cm As_2S_3 waveguide [Figure 14(b)] for creating UWB pulses.

In addition to high Kerr nonlinearities, the same As_2S_3 waveguide has been shown to support gigahertz-frequency acoustic modes. This gives rise to another nonlinear effect, SBS (as described earlier), which is usually observed in long silica fibers. SBS manifests itself as a megahertz-width gain resonance at a downshifted frequency (typically 7–11 GHz) from an optical pump. Harnessing this nonlinear phenomena in centimeter-scale optical waveguides (instead of several kilometers of optical fibers) has led to miniaturization of key MWP functionalities, including tunable delay lines [122], tunable RF phase shifters [123], and high-performance bandpass filters [124]. The most important outcome based on SBS in chalcogenide, however, has been high-quality tunable bandstop filters with ultrahigh suppression [79]. Such filters exhibit a bandstop suppression of 55 dB, a quality factor of 375 at 30 GHz, and 2,900% fractional tuning range [Figure 14(c)].

Concluding Remarks: Outlook and Vision

The field of IMWP is now one of the most active and exciting areas within MWP, as evidenced by the growing number of papers being published. The motivation for this development of IMWP is the number of growing and emerging applications of MWP technology in general; this includes, e.g., the developments in ROF for 5G.

For the field of IMWP to eventually flourish and find widespread application, an ecosystem similar to that of MMIC technology will be required, in which foundry-level fabrication and modeling, along with computer-aided design (CAD) testing, measurement, and packaging all go hand in hand. The major challenge here is the presence of both microwave and photonic devices and signals within the same chip or subsystem. Looking at commercial CAD packages, e.g., we see very sophisticated microwave simulators, and the same will be required for photonics. However, a unified microwave photonic CAD package with comprehensive microwave and photonic models does not really exist, except in the sense of using the concept of cosimulation between existing microwave and photonic CAD programs.

In principle, microwave photonic measurements are at a somewhat more advanced stage, both for digital and analog cases. Although an accepted universal definition of scattering parameters has yet to be standardized for

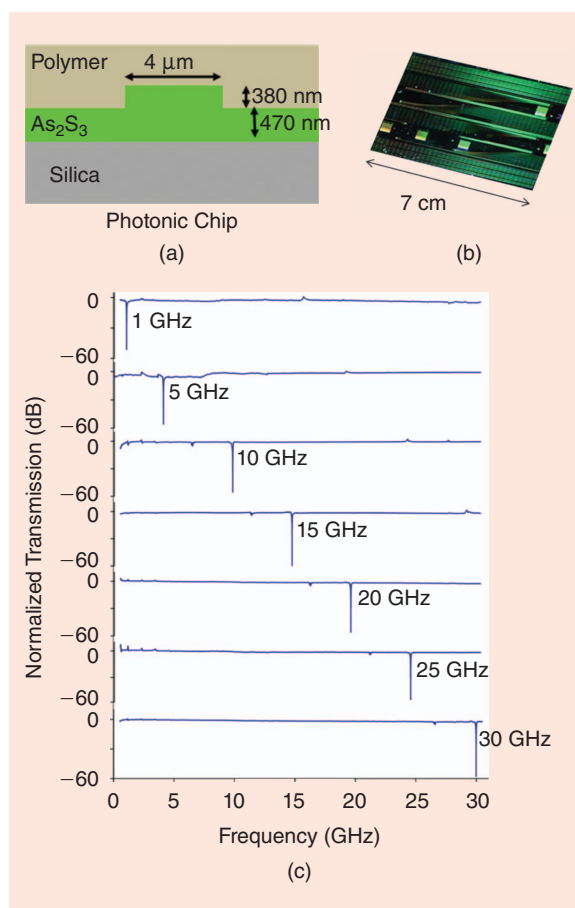


Figure 14. (a) The schematic of a 16×1 optical beamforming chip. (b) The mask layout. (c) The photograph of a processed wafer. (d) The packaged chip with electrical connections and fiber pigtailed. (Figure adapted from [113] courtesy of the Optical Society.)

IMWP, there are well-established techniques for measurements such as small-signal modulation response of modulators and photodiodes, for example [125]. In addition, optical fiber probing of wafers is a routine operation; hence, we see the characterization part of the equation as being well developed.

One of the disadvantages of integrated photonics in general compared with integrated electronics is that the latter has the flexibility afforded by the transistor, a device that can be used to design a multitude of different circuits and functions. In contrast, no such “universal” device exists in photonics, although there has been interesting work done recently on homogeneous integration of transistors and lasers [126], [127]. The recent proposal for a “microwave photonic transistor” [128] (which, in essence, is an analog signal processing engine as outlined in Figure 4) may well act as a spur for focused development of IMWP applications.

Comparing MMIC technology with IMWP, the former is simpler in the sense that it allows for planar (or multilevel) integration on a single material (such as GaAs, InP, and RF-CMOS), while the latter must

accommodate different functions, such as optical coupling and RF inputs/outputs, and the optimal material for various photonic functions (lasing, modulation, photodetection) differs from device to device. The holy grail of IMWP would be a material system that supports monolithic integration of active and passive microwave components as well as active and passive photonic components while simultaneously achieving high performance with respect to the various requirements placed on the components. For the moment, such a technology is elusive.

Integration platforms, whether they be monolithic or hybrid, have many varieties. This creates challenges, but there has been some convergence, at least for SiPh, in that a standard platform is imminent and soon SiPh will become almost a commodity. In this respect, SiPh is regarded as the best “compromise” candidate in that it builds upon the vast infrastructure in regular silicon electronics. However, it is only in recent years that we have seen the emergence of the foundry concept in SiPh; hence, there is still some way to go before we see the emergence of an IMWP foundry with all the associated features, such as element libraries and design and test methodologies.

A major challenge with SiPh is that the waveguides cannot support much optical power, so this technology will only be suitable for certain applications, or at least for some parts of MWP systems. In addition, in many application cases, the optimal solution may be provided by hybrid electronics–photronics integration, merging MMICs and IMWP circuits in a single package, similar to the architecture of optical communication transceivers. Possibly, IMWP systems could benefit from a similar approach, such as that being pursued for high-speed active optical cables, with the limitation that silicon photonics and CMOS electronics used in interconnects will probably not be the best solution for MWP, and a different platform could be the optimal one. For MWP, higher on-chip optical power would be required for some applications, so small silicon waveguides may not work.

Despite the ongoing technical challenges and the lack of convergence toward a single integrative approach that would cover all required passive and active functionalities, the field of IMWP is expected to continue its rapid development, including the investigation of relatively new material systems such as chalcogenide and graphene; the latter, in particular, is receiving much attention worldwide due to its unique properties, including low-cost fabrication, high-frequency electronics properties (due to high carrier mobility), and an inherent 2-D nature that lends itself to quantum confinement. A number of modulators have been reported, although, for the moment, the bandwidths have been limited to a few gigahertz [129]; much of the activity with graphene is currently focused on the terahertz region and includes demonstrations of such functions as switching, amplification, and phase shifting [130].

References

- [1] J. Capmany and D. Novak, “Microwave photonics combines two worlds,” *Nat. Photonics*, vol. 1, no. 6, pp. 319–330, 2007.
- [2] A. Seeds, “Microwave photonics,” *IEEE Trans. Microwave Theory Tech.*, vol. 50, no. 3, pp. 877–887, 2002.
- [3] J. Yao, “Microwave photonics,” *IEEE J. Lightwave Technol.*, vol. 27, no. 3, pp. 314–335, 2009.
- [4] S. Iezekiel, Ed., *Microwave Photonics: Devices and Applications*. Hoboken, NJ: Wiley, 2009.
- [5] “Technology focus on microwave photonics,” *Nat. Photonics*, vol. 5, no. 12, pp. 723–736, Dec. 2011.
- [6] C. H. Cox III, *Analog Optical Links: Theory and Practice*. Cambridge, U.K.: Cambridge Univ. Press, 2006.
- [7] H. Al-Raweshidi and S. Komaki, Eds. *Radio Over Fiber Technologies for Mobile Communications Networks*. Boston, MA: Artech House, 2002.
- [8] M. Mjeku and N. J. Gomes, “Performance analysis of 802.11e transmission bursting in fiber-fed networks,” in *Proc. Radio Wireless Symp.*, 2008, pp. 133–136.
- [9] M. Sotom, B. Benazet, A. Le Kerneec, and M. Maignan, “Microwave photonic technologies for flexible satellite telecom payloads,” in *Proc. 35th European Conf. Optical Communication*, Vienna, 2009, pp. 1–4.
- [10] M. Crisp, R. V. Penty, I. H. White, and A. Bell, “Wideband radio over fiber distributed antenna systems for energy efficient in-building wireless communications,” in *Proc. IEEE 71st Vehicular Technology Conf.*, Taipei, Taiwan, 2010, pp. 1–5.
- [11] J. Capmany, B. Ortega, and D. Pastor, “A tutorial on microwave photonic filters,” *J. Lightwave Technol.*, vol. 24, no. 1, pp. 201–229, 2006.
- [12] M. Popov, “The convergence of wired and wireless services delivery in access and home networks,” in *Proc. Conf. Optical Fiber Communication*, 2010.
- [13] A. M. J. Koonen, A. M. Koonen, M. G. Larrode, A. Ng’oma, K. Wang, H. Yang, Y. Zheng, and E. Tangdiongga, “Perspectives of radio-over-fiber technologies,” presented at the Conf. Optical Fiber Communication, 2008, Paper OThP3.
- [14] D. D. Arnone, C. M. Ciesla, A. Corchia, S. Egusa, M. Pepper, J. M. Chamberlain, C. Bezzant, E. H. Linfield, R. Clothier, and N. Khammo, “Applications of terahertz (THz) technology to medical imaging,” in *Proc. Int. Society Optics Photonics, Industrial Lasers Inspection (EUROPTO Series)*, 1999.
- [15] S. Movassaghi, M. Abolhasan, J. Lipman, D. Smith, and A. Jamalipour, “Wireless body area networks: A survey,” *IEEE Commun. Surveys Tuts*, vol. 16, no. 3, pp. 1658–1686, 2014.
- [16] A. Luigi, A. Iera, and G. Morabito, “The internet of things: A survey,” *Comput. Netw.*, vol. 54, no. 15, pp. 2787–2805, 2010.
- [17] (2015, June 28). S to Q-band RF photonic links 3–50 GHz, pharad. [Online]. Available: <http://www.pharad.com/s-q-band-rf-photonic-link.html>
- [18] A. Perentos, F. Cuesta-Soto, M. Rodrigo, A. Canciamilla, B. Vidal, L. Pierno, A. Griol, N. S. Losilla, L. Bellieres, F. Lopez-Royo, A. Meloni, and S. Iezekiel, “Variable carrier reduction in radio-over-fiber systems for increased modulation efficiency using a Si₃N₄ tunable extinction ratio ring resonator,” *Opt. Express*, vol. 20, no. 23, pp. 25478–25488, 2012.
- [19] D. Marpaung, C. Roeloffzen, A. Leinse, and M. Hoekman, “A photonic chip based frequency discriminator for a high performance microwave photonic link,” *Opt. Express*, vol. 18, no. 26, pp. 27359–27370, 2010.
- [20] D. J. Blumenthal, J. Barton, N. Beheshti, J. E. Bowers, E. Burmeister, L. A. Coldren, M. Dummer, G. Epps, A. Fang, Y. Ganjali, J. Garcia, B. Koch, V. Lal, E. Lively, J. Mack, M. Masanovic, N. McKeown, K. Nguyen, S. C. Nicholes, H. Park, B. Stamenic, A. Tauke-Pedretti, H. Poulsen, and M. Sysak, “Integrated photonics for low-power packet networking,” *IEEE J. Select. Topics Quantum Electron.*, vol. 17, no. 2, pp. 458–471, 2011.
- [21] S. Ayling, D. Wight, D. M. Allenson, K. Hilton, and G. Smith, “Intrinsically matched 50 ohm laser arrays with greater than 100% quantum efficiencies for optically coupled transistors and low loss fiber optic links,” in *Proc. SPIE—Int. Society Optical Engineering*, 1998, pp. 199–208.
- [22] D. Marpaung, C. Roeloffzen, R. Heideman, A. Leinse, S. Sales, and J. Capmany, “Integrated microwave photonics,” *Laser Photon. Rev.*, vol. 7, no. 4, pp. 506–538, 2013.
- [23] R. J. Mailloux, *Phased Array Antenna Handbook*. Boston, MA: Artech House, 2005.

- [24] R. E. Collin, *Antennas and Radiowave Propagation*. New York: McGraw-Hill, 1985.
- [25] T. Berceci and P. Herczfeld, "Microwave photonics—A historical perspective," *IEEE Trans. Microwave Theory Tech.*, vol. 58, no. 11, pp. 2992–3000, 2010.
- [26] R. A. Soref, "Programmable time-delay devices," *Appl. Opt.*, vol. 23, no. 21, pp. 3736–3737, 1984.
- [27] A. P. Goutzoulis, D. Davies, and J. Zomp, "Prototype binary fiber optic delay line," *Opt. Eng.*, vol. 28, no. 11, pp. 1193–1202, 1989.
- [28] F. Soares, "Photonic integrated true-time-delay beamformers in InP technology," Ph.D. dissertation, Dept. Electr. Eng., Eindhoven Univ. Technol., Eindhoven, The Netherlands, Sept. 2006.
- [29] W. Ng, A. A. Walston, G. L. Tangonan, J. J. Lee, I. L. Newberg, and N. Bernstein, "The first demonstration of an optically steered microwave phased array antenna using true-time-delay," *J. Lightwave Technol.*, vol. 9, no. 9, pp. 1124–1131, 1991.
- [30] A. Goutzoulis, K. Davies, J. Zomp, P. Hrycak, and A. Johnson, "Development and field demonstration of a hardware-compressive fiber-optic true-time-delay steering system for phased-array antennas," *Appl. Opt.*, vol. 33, no. 35, pp. 8173–8185, 1994.
- [31] N. A. Riza, *Selected Papers On Photonic Control Systems for Phased Array Antennas*, vol. MS136. Bellingham, WA: SPIE Press, 1997.
- [32] R. J. Mailloux, *Phased Array Antenna Handbook*. Boston, MA: Artech House, 2005.
- [33] E. Ackerman, S. Wanuga, D. Kasemset, W. Minford, N. Thorsten, and J. Watson, "Integrated 6-bit photonic true-time-delay unit for lightweight 3-6 GHz radar beamformer," in *IEEE MTT-S Int. Microwave Symp. Dig.*, 1992, pp. 681–684.
- [34] D. T. K. Tong and M. C. Wu, "Multiwavelength optically controlled phased-array antennas," *IEEE Trans. Microwave Theory Tech.*, vol. 46, no. 1, pp. 108–115, 1998.
- [35] M. Burla, D. Marpaung, L. Zhuang, C. Roeloffzen, M. R. Khan, A. Leinse, M. Hoekman, and R. Heideman, "On-chip CMOS compatible reconfigurable optical delay line with separate carrier tuning for microwave photonic signal processing," *Opt. Express*, vol. 19, no. 22, pp. 21475–21484, 2011.
- [36] M. Burla, "Advanced integrated optical beam forming networks for broadband phased array antenna systems," Ph.D. dissertation, CTIT, Univ. Twente, Enschede, The Netherlands, 2013.
- [37] Y. Chen, K. Wu, F. Zhao, and R. T. Chen, "Loss compensated photonic true-time delay for phased-array antenna," in *Proc. IEEE Antennas Propagation Society Int. Symp.*, 2004, vol. 4, pp. 4324–4327.
- [38] X. Wang, B. Howley, M. Y. Chen, P. Basile, and R. T. Chen, "Fully-integrated 4-bit true time delay module using polymer optical switches and waveguide delay lines," presented at the Integrated Photonics Research Applications, Optical Society America, 2006. Paper IMF4.
- [39] Y. Chen, K. Wu, F. Zhao, G. Kim, and R. T. Chen, "Reconfigurable true-time delay for wideband phased-array antennas," in *Proc. SPIE*, 2004, vol. 5363, pp. 125–130.
- [40] K. Horikawa, I. Ogawa, H. Ogawa, and T. Kitoh, "Photonic switched true time delay beam forming network integrated on silica waveguide circuits," in *IEEE MTT-S Int. Microwave Symp. Dig.*, 1995, pp. 65–68.
- [41] K. Horikawa, I. Ogawa, T. Kitoh, and H. Ogawa, "Silica-based integrated planar lightwave true-time-delay network for microwave antenna applications," in *Proc. Optical Fiber Communications*, 1996. pp. 100–101.
- [42] J. LeGrange, A. Kasper, C. Madsen, M. Cappuzzo, E. Chen, A. Griffin, E. Laskowski, and M. Rasras, "Demonstration of an integrated, tunable high resolution true time delay line," in *Proc. 17th Annu. Meeting IEEE Lasers Electro-Optics Society*, 2004, vol. 2, pp. 790–791.
- [43] M. S. Rasras, C. K. Madsen, M. A. Cappuzzo, E. Chen, L. T. Gomez, E. J. Laskowski, A. Griffin, A. Wong-Foy, A. Gasparyan, A. Kasper, J. LeGrange, and S. S. Pastel, "Integrated resonance-enhanced variable optical delay lines," *IEEE Photon. Technol. Lett.*, vol. 17, no. 4, pp. 834–836, 2005.
- [44] K. Horikawa, Y. Nakasuga, and H. Ogawa, "Self-heterodyning optical waveguide beam forming and steering network integrated on Lithium Niobate substrate," *IEEE Trans. Microwave Theory Tech.*, vol. 43, no. 9, pp. 2395–2401, 1995.
- [45] W. W. Ng, D. Yap, A. A. Narayanan, T. P. Liu, and R. R. Hayes, "GaAs and silica-based integrated optical time-shift network for phased arrays," in *SPIE Proc.*, 1994, vol. 2155, pp. 114–123.
- [46] W. Ng, D. Yap, A. Narayanan, and A. Walston, "High-precision detector-switched monolithic GaAs time-delay network for the optical control of phased arrays," *IEEE Photon. Technol. Lett.*, vol. 6, no. 2, pp. 231–234, 1994.
- [47] J. Stulemeijer, F. van Vliet, K. Benoist, D. Maat, and M. Smit, "Compact photonic integrated phase and amplitude controller for phased-array antennas," *IEEE Photon. Technol. Lett.*, vol. 11, no. 1, pp. 122–124, 1999.
- [48] G. Flamand, K. de Mesel, I. Moerman, B. Dhoedt, W. Hunziker, A. Kalmar, R. Baets, P. van Daele, and W. Leeb, "InP-based pic for an optical phased-array antenna at 1.06 μm ," *IEEE Photon. Technol. Lett.*, vol. 12, no. 7, pp. 876–878, 2000.
- [49] L. M. Renan, G. John, L. Wenzao, B. Jared, S. B. Jonathon, J. R. H. Martijn, J. E. Bowers, and D. J. Blumenthal, "Integrated ultra-low-loss 4-bit tunable delay for broadband phased array antenna applications," *IEEE Photon. Technol. Lett.*, vol. 25, no. 12, pp. 1165–1168, 2013.
- [50] G. Agrawal, *Nonlinear Fiber Optics*. New York: Elsevier Science, 2012.
- [51] R. D. Esman, M. Y. Frankel, J. Dexter, L. Goldberg, M. Parent, D. Stilwell, and D. Cooper, "Fiber-optic prism true time-delay antenna feed," *IEEE Photon. Technol. Lett.*, vol. 5, no. 11, pp. 1347–1349, 1993.
- [52] M. Y. Frankel, P. J. Matthews, and R. D. Esman, "Fiber-optic true time steering of an ultra wide-band receive array," *IEEE Trans. Microwave Theory Tech.*, vol. 45, no. 8, pp. 1522–1526, 1997.
- [53] P. J. Matthews, M. Y. Frankel, and R. D. Esman, "A wide-band fiber-optic true-time-steered array receiver capable of multiple independent simultaneous beams," *IEEE Photon. Technol. Lett.*, vol. 10, no. 5, pp. 722–724, 1998.
- [54] M. Y. Frankel and R. D. Esman, "True time-delay fiber-optic control of an ultrawideband array transmitter/receiver with multi-beam capability," *IEEE Trans. Microwave Theory Tech.*, vol. 43, no. 9, pp. 2387–2394, 1995.
- [55] M. Y. Frankel, R. Esman, and M. Parent, "Array transmitter/receiver controlled by a true time-delay fiber-optic beamformer," *IEEE Photon. Technol. Lett.*, vol. 7, no. 10, pp. 1216–1218, 1995.
- [56] J. Roman, M. Frankel, P. Matthews, and R. Esman, "Time-steered array with a chirped grating beamformer," *Electron. Lett.*, vol. 33, no. 8, pp. 652–653, 1997.
- [57] J. Medberry, P. Biernacki, and P. Matthews, "Range demonstration of an ultra-wideband, continuous, time steered array using a fiber-optic, cascaded grating prism," in *IEEE MTT-S Int. Microwave Symp. Dig.*, 2000, vol. 1, pp. 597–600.
- [58] I. Giuntoni, D. Stolarek, D. I. Kroushkov, J. Bruns, L. Zimmermann, B. Tillack, and K. Petermann, "Continuously tunable delay line based on SOI tapered Bragg gratings," *Opt. Express*, vol. 20, no. 10, pp. 11241–11246, 2012.
- [59] M. K. Smit, "New focusing and dispersive planar component based on an optical phased array," *Electron. Lett.*, vol. 24, no. 7, pp. 385–386, 1988.
- [60] S. Yegnanarayanan, P. Trinh, and B. Jalali, "Recirculating photonic filter: A wavelength-selective time delay for phased-array antennas and wavelength code-division multiple access," *Opt. Lett.*, vol. 21, no. 10, pp. 740–742, 1996.
- [61] T. Koonen and Z. Cao, "Optically controlled 2D radio beam steering system," in *Proc. Asia-Pacific Microwave Photonics Conf. Int. Topical Meeting Microwave Photonics*, Oct. 20–23, 2014, pp. 389–391.
- [62] B. Jalali and S. Yegnanarayanan, "Optically controlled phased-array antenna using wavelength-selective true time delay," in *Proc. IEEE Int. Conf. Phased Array Systems Technology*, 2000, pp. 367–370.
- [63] B. Vidal, D. Madrid, J. Coffal, and J. Marti, "Novel photonic true-time-delay beamformer based on the free-spectral-range periodicity of arrayed waveguide gratings and fiber dispersion," *IEEE Photon. Technol. Lett.*, vol. 14, no. 11, pp. 1614–1616, 2002.
- [64] J. Sancho, J. Bourderionnet, J. Lloret, S. Combr e, I. Gasulla, S. Xavier, S. Sales, P. Colman, G. Lhoucq, D. Dolfi, J. Capmany, and

- A. de Rossi, "Integrable microwave filter based on a photonic crystal delay line," *Nature Commun.*, vol. 3, p. 1075, Sept. 2012.
- [65] L. Zhuang, C. Roeloffzen, R. Heideman, A. Borremans, A. Meijerink, and W. van Etten, "Single-chip ring resonator-based 1×8 optical beam forming network in CMOS-compatible waveguide technology," *IEEE Photon. Technol. Lett.*, vol. 19, no. 15, pp. 1130–1132, 2007.
- [66] J. Cardenas, M. A. Foster, N. Sherwood-Droz, C. B. Poitras, H. L. R. Lira, B. Zhang, A. L. Gaeta, J. B. Khurgin, P. Morton, and M. Lipson, "Wide-bandwidth continuously tunable optical delay line using silicon microring resonators," *Opt. Express*, vol. 18, no. 25, pp. 26525–26534, 2010.
- [67] P. A. Morton, J. Cardenas, J. B. Khurgin, and M. Lipson, "Fast thermal switching of wideband optical delay line with no long-term transient," *IEEE Photon. Technol. Lett.*, vol. 24, no. 6, pp. 512–514, 2012.
- [68] A. Meijerink, C. G. H. Roeloffzen, R. Meijerink, L. Zhuang, D. A. I. Marpaung, M. J. Benthum, M. Burla, J. Verpoorte, P. Jorna, A. Hulzinga, and W. van Etten, "Novel ring resonator-based integrated photonic beamformer for broadband phased array receive antennas—Part I: Design and performance analysis," *J. Lightwave Technol.*, vol. 28, no. 1, pp. 3–18, 2010.
- [69] L. Zhuang, C. G. H. Roeloffzen, A. Meijerink, M. Burla, D. A. I. Marpaung, A. Leinse, M. Hoekman, R. G. Heideman, and W. van Etten, "Novel ring resonator-based integrated photonic beamformer for broadband phased array receive antennas—Part II: Experimental prototype," *J. Lightwave Technol.*, vol. 28, no. 1, pp. 19–31, 2010.
- [70] D. Marpaung, L. Zhuang, M. Burla, C. Roeloffzen, J. Verpoorte, H. Schippers, A. Hulzinga, P. Jorna, W. Beeker, A. Leinse, R. Heideman, B. Noharet, Q. Wang, B. Sanadgol, and R. Baggen, "Towards a broadband and squint-free Ku-band phased array antenna system for airborne satellite communications," in *Proc. 5th European Conf. Antennas Propagation*, Rome, Italy, 2011, pp. 2623–2627.
- [71] D. Marpaung, L. Zhuang, M. Burla, C. Roeloffzen, B. Noharet, Q. Wang, W. Beeker, A. Leinse, and R. Heideman, in *Proc. IEEE Topical Meeting Microwave Photonics Asia Pacific Microwave Photonics*, Singapore, Oct. 18–21, 2011, pp. 458–461.
- [72] M. Burla, C. G. H. Roeloffzen, L. Zhuang, D. Marpaung, M. R. Khan, P. Maat, D. Dijkstra, A. Leinse, M. Hoekman, and R. Heideman, "System integration and radiation pattern measurements of a phased array antenna employing an integrated photonic beamformer for radio astronomy applications," *Appl. Opt.*, vol. 51, no. 7, pp. 789–802, 2012.
- [73] L. Zhuang, D. Marpaung, M. Burla, W. Beeker, A. Leinse, and C. Roeloffzen, "Low-loss, high-index-contrast $\text{Si}_3\text{N}_4/\text{SiO}_2$ optical waveguides for optical delay lines in microwave photonics signal processing," *Opt. Express*, vol. 19, no. 23, pp. 23162–23170, 2011.
- [74] M. Burla, D. Marpaung, L. Zhuang, A. Leinse, M. Hoekman, R. Heideman, and C. Roeloffzen, "Integrated photonic Ku-band beamformer chip with continuous amplitude and delay control," *IEEE Photon. Technol. Lett.*, vol. 25, no. 12, pp. 1145–1148, June 15, 2013.
- [75] M. Burla, D. A. I. Marpaung, L. Zhuang, M. R. Khan, A. Leinse, W. Beeker, M. Hoekman, R. G. Heideman, and C. G. H. Roeloffzen, "Multiwavelength-integrated optical beamformer based on wavelength division multiplexing for 2-D phased array antennas," *J. Lightwave Technol.*, vol. 32, no. 20, pp. 3509–3520, Oct. 15, 2014.
- [76] G. Grosskopf, R. Eggemann, H. Ehlers, A. Kortke, B. Kuhlow, G. Przyrembel, D. Rohde, and S. Zinal, "Maximum directivity beamformer at 60 GHz with optical feeder," *IEEE Trans. Antennas Propagat.*, vol. 51, no. 11, pp. 3040–3046, 2003.
- [77] M. Burla, L. R. Cortés, M. Li, X. Wang, L. Chrostowski, and J. Azaña, "On-chip programmable ultra-wideband microwave photonic phase shifter and true time delay unit," *Opt. Lett.*, vol. 39, no. 21, pp. 6181–6184, 2014.
- [78] D. Marpaung, M. Pagani, B. Morrison, and B. Eggleton, "Nonlinear integrated microwave photonics," *J. Lightwave Technol.*, vol. 32, no. 20, pp. 3421–3427, 2014.
- [79] D. Marpaung, B. Morrison, M. Pagani, R. Pant, D. Choi, B. Luther-Davies, S. Madden, and B. Eggleton, "Low-power, chip-based stimulated Brillouin scattering microwave photonic filter with ultrahigh selectivity," *Optica*, vol. 2, no. 2, pp. 76–83, 2015.
- [80] M. Pagani, D. Marpaung, and B. Eggleton, "Ultra-wideband microwave photonic phase shifter with configurable amplitude response," *Opt. Lett.*, vol. 39, no. 20, pp. 5854–5857, 2014.
- [81] Y. Zhang, H. Wu, D. Zhu, and S. Pan, "An optically controlled phased array antenna based on single sideband polarization modulation," *Opt. Express*, vol. 22, no. 4, pp. 3761–3765, 2014.
- [82] R. Bonjour, S. A. Gebrewold, D. Hillerkuss, C. Hafner, and J. Leuthold, "Ultra-fast tunable true-time delay using complementary phase shifted spectra (CPSS)," presented at the Proc. OFC, 2015, Paper W2A.67.
- [83] J. Wang, H. Shen, L. Fan, R. Wu, B. Niu, L. T. Varghese, Y. Xuan, D. E. Leaird, X. Wang, F. Gan, A. M. Weiner, and M. Qi, "Reconfigurable radio-frequency arbitrary waveforms synthesized in a silicon photonic chip," *Nature Commun.*, vol. 6, article 5957, 2015.
- [84] C. H. Henry, G. E. Blonder, and R. F. Kazarinov, "Glass waveguides on silicon for hybrid optical packaging," *J. Lightwave Technol.*, vol. 7, no. 10, pp. 1530–1539, 1989.
- [85] S. Iezekiel, E. A. Soshea, M. F. O'Keefe, and M. S. Christopher, "Microwave photonic multichip modules packaged on a glass-silicon substrate," *IEEE Trans. Microwave Theory Tech.*, vol. 43, no. 9, pp. 2421–2427, 1995.
- [86] K. J. Tae, J. J. Ju, P. S. Sontak, P. S. Koo, M.-S. Kim, and L. Myung-Hyun, "Electric-circuit-embedded polymer optical bench," *IEEE Photon. Technol. Lett.*, vol. 19, no. 5, pp. 318–320, 2007.
- [87] H. N. Klein, H. Chen, D. Hoffman, A. G. Steffan, and K. O. Velthaus, "1.55mm Mach-Zehnder modulators on InP for optical 40/80 Gbit/s transmission networks," presented at the Int. Conf. Indium Phosphide Related Materials, 2006, Paper TuA2.4.
- [88] S. Dogru and N. Dagli, "Traveling wave electrodes for wide-bandwidth substrate-removed electro-optic modulators," presented at the IEEE Photonics Conf., 2012, Paper MS5.
- [89] J. S. Barton, E. J. Skogen, M. L. Masanovic, S. P. DenBaars, and L. A. Coldren, "A widely tunable high-speed transmitter using an integrated SGDBR laser-semiconductor optical amplifier and Mach-Zehnder modulator," *IEEE J. Select. Topics Quantum Electron.*, vol. 9, no. 5, pp. 1113–1117, 2003.
- [90] M. M. Dummer, J. R. Raring, J. Klamkin, A. Tauke-Pedretti, and L. A. Coldren, "Selectively-undercut traveling-wave electroabsorption modulators incorporating a p-InGaAs contact layer," *Opt. Express*, vol. 16, no. 25, pp. 20388–20394, 2008.
- [91] M. M. Dummer, J. Klamkin, A. Tauke-Pedretti, and L. A. Coldren, "40 Gb/s field-modulated wavelength converters for all-optical packet switching," *IEEE J. Select. Topics Quantum Electron.*, vol. 15, no. 3, pp. 494–503, 2009.
- [92] F. M. Soares, K. Janiak, J. Kreissl, M. Moehrl, and N. Grote, "Semi-insulating substrate based generic InP photonic integration platform," in *Proc. SPIE Integrated Photonics: Materials, Devices, and Applications II*, 2013, vol. 8767.
- [93] N. Li, X. Li, S. Demiguel, X. Zheng, J. C. Campbell, D. A. Tulchinsky, K. J. Williams, T. D. Isshiki, G. S. Kinsey, and R. Sudharsanan, "High-saturation-current charge-compensated InGaAs-InP uni-traveling-carrier photodiode," *IEEE Photon. Technol. Lett.*, vol. 16, no. 3, pp. 864–866, 2004.
- [94] J. Klamkin, A. Ramaswamy, L. A. Johansson, H.-F. Chou, M. N. Sysak, J. R. Raring, N. Parthasarathy, S. P. DenBaars, J. E. Bowers, and L. A. Coldren, "High output saturation and high-linearity uni-traveling-carrier waveguide photodiodes," *IEEE Photon. Technol. Lett.*, vol. 19, no. 3, pp. 149–151, 2007.
- [95] J. Klamkin, S. M. Madison, D. C. Oakley, A. Napoleone, F. J. O'Donnell, M. Sheehan, L. J. Missaggia, J. M. Caissie, J. J. Plant, and P. W. Juodawlkis, "Uni-traveling-carrier variable confinement waveguide photodiodes," *Opt. Express*, vol. 19, no. 11, pp. 10199–10205, 2011.
- [96] A. Ramaswamy, L. A. Johansson, J. Klamkin, H.-F. Chou, C. Sheldon, M. J. Rodwell, L. A. Coldren, and J. E. Bowers, "Integrated coherent receivers for high-linearity microwave photonic links," *J. Lightwave Technol.*, vol. 26, no. 1, pp. 209–216, 2008.
- [97] M. K. Smit, X. Leijtens, E. Bente, J. van der Tol, H. Ambrosius, D. Robbins, M. J. Wale, N. Grote, and M. Schell, "A generic foundry

- model for InP-based photonic ICs," present at the Optical Fiber Communication Conf., 2012, Paper OM3E.3.
- [98] M. Smit, X. Leijts, H. Ambrosius, E. Bente, J. van der Tol, B. Smalbrugge, T. de Vries, E.-J. Geluk, J. Bolk, R. van Veldhoven, L. Augustin, P. Thijs, D. D'Agostino, H. Rabbani, K. Lawniczuk, S. Stopinski, S. Tahvili, A. Corradi, E. Kleijn, D. Dzubrou, M. Felicetti, E. Bitincka, V. Moskalenko, J. Zhao, R. Santos, G. Gilardi, W. Yao, K. Williams, P. Stabile, P. Kuindersma, J. Pello, S. Bhat, Y. Jiao, D. Heiss, G. Roelkens, M. Wale, P. Firth, F. Soares, N. Grote, M. Schell, H. Debregeas, M. Achouche, J.-L. Gentner, A. Bakker, T. Korthorst, D. Gallagher, A. Dabbs, A. Melloni, F. Morichetti, D. Melati, A. Wonfor, R. Pentyl, R. Broeke, R. Musk, and D. Robbins, "An introduction to InP-based generic integration technology," *Semicond. Sci. Technol.*, vol. 28, no. 8, p. 083001, 2014.
- [99] F. Kish, R. Nagarajan, D. Welch, P. Evans, J. Rossi, J. Pleumeekers, A. Dentai, M. Kato, S. Corzine, R. Muthiah, M. Ziari, R. Schneider, M. Reffle, T. Butrie, D. Lambert, M. Missey, V. Lal, M. Fisher, S. Murthy, R. Salvatore, S. Demars, A. James, and C. Joyner, "From visible light-emitting diodes to large-scale III-V photonic integrated circuits," *Proc. IEEE*, vol. 101, p. 2255, Oct. 2013.
- [100] A. W. Fang, H. Park, O. Cohen, R. Jones, M. J. Paniccia, and J. E. Bowers, "Electrically pumped hybrid AlGaInAs-Silicon evanescent laser," *Opt. Express*, vol. 14, no. 20, pp. 9203–9210, 2006.
- [101] M. R. Watts, W. A. Zortman, D. C. Trotter, R. W. Young, and A. L. Lentine, "Low-voltage, compact, depletion-mode silicon Mach-Zehnder modulator," *IEEE J. Select. Topics Quantum Electron.*, vol. 16, no. 1, pp. 159–164, 2010.
- [102] G. Li, X. Zheng, J. Yao, H. Thacker, I. Shubin, Y. Luo, K. Raj, J. E. Cunningham, and A. V. Krishnamoorthy, "25Gb/s 1V-driving CMOS ring modulator with integrated thermal tuning," *Opt. Express*, vol. 19, no. 21, pp. 20435–20443, 2011.
- [103] A. Ayazi, T. Baehr-Jones, Y. Liu, A. E.-J. Lim, and M. Hochberg, "Linearity of silicon ring modulators for analog optical links," *Opt. Express*, vol. 20, no. 12, pp. 13115–13122, 2012.
- [104] L. Vivien, J. Osmond, J.-M. Féféli, D. Marris-Morini, P. Crozat, J.-F. Damlencourt, E. Cassan, Y. Lecunff, and S. Laval, "42 GHz p.i.n germanium photodetector integrated in a silicon-on-insulator waveguide," *Opt. Express*, vol. 17, no. 8, pp. 6252–6257, 2009.
- [105] A. Ramaswamy, M. Piels, N. Nunoya, T. Yin, and J. E. Bowers, "High power silicon-germanium photodiodes for microwave photonic applications," *IEEE Trans. Microwave Theory Tech.*, vol. 58, no. 11, pp. 3336–3343, 2010.
- [106] J. Lloret, J. Sancho, M. Pu, I. Gasulla, K. Yvind, S. Sales, and J. Capmany, "Tunable complex-valued multi-tap microwave photonic filter based on single silicon-on-insulator microring resonator," *Opt. Express*, vol. 19, no. 13, pp. 12402–12407, 2011.
- [107] H.-W. Chen, A. W. Fang, J. D. Peters, Z. Wang, J. Bovington, D. Liang, and J. E. Bowers, "Integrated microwave photonic filter on a hybrid silicon platform," *IEEE Trans. Microwave Theory Tech.*, vol. 58, no. 11, pp. 3213–3219, 2010.
- [108] T. Aalto, M. Cherchi, M. Harjanne, S. Ylänen, M. Kapulainen, and T. Vehmas, "Launching of multi-project wafer runs in ePIXfab with micron-scale silicon rib waveguide technology," presented at the SPIE, 2014, vol. 8990.
- [109] M. J. R. Heck, J. F. Bauters, M. L. Davenport, J. K. Doylend, S. Jain, G. Kurczveil, S. Srinivasan, Y. Tang, and J. E. Bowers, "Hybrid silicon photonic integrated circuit technology," *IEEE J. Select. Topics Quantum Electron.*, vol. 20, no. 4, p. 6100117, 2013.
- [110] R. G. Heideman, D. H. Geuzebroek, A. Leinse, A. Melloni, F. Morichetti, C. Roeloffzen, A. Meijerink, L. Zhuang, W. van Etten, E. Klein, and A. Driessen, "Low loss, high contrast optical waveguides based on CMOS compatible LPCVD processing," presented at the 13th European Conf. Integrated Optics (ECIO), Copenhagen, Denmark, 2007, Paper WB0.
- [111] F. Morichetti, A. Melloni, M. Martinelli, R. G. Heideman, A. Leinse, D. H. Geuzebroek, and A. Borreman, "Box-shaped dielectric waveguides: A new concept in integrated optics?" *J. Lightwave Technol.*, vol. 25, no. 9, pp. 2579–2589, 2007.
- [112] (2015, June 28). LioniX BV. [Online]. Available: <http://www.lionixbv.nl>
- [113] C. Roeloffzen, L. Zhuang, C. Taddei, A. Leinse, R. Heideman, P. van Dijk, R. Oldenbeuving, D. Marpaung, M. Burla, and K. Boller, "Silicon nitride microwave photonic circuits," *Opt. Express*, vol. 21, no. 19, pp. 22937–22961, 2013.
- [114] R. Heideman, M. Hoekman, and E. Schreuder, "TriPleX-based integrated optical ring resonators for lab-on-a-chip and environmental detection," *IEEE J. Select. Topics Quantum Electron.*, vol. 18, no. 5, pp. 1583–1596, 2012.
- [115] J. F. Bauters, M. J. R. Heck, D. John, D. Dai, M.-C. Tien, J. S. Barton, A. Leinse, R. G. Heideman, D. J. Blumenthal, and J. E. Bowers, "Ultra-low-loss high-aspect-ratio Si₃N₄ waveguides," *Opt. Express*, vol. 19, no. 4, pp. 3163–3174, 2011.
- [116] J. Capmany, B. Ortega, and D. Pastor, "A tutorial on microwave photonic filters," *J. Lightwave Technol.*, vol. 24, no. 1, pp. 201–229, 2006.
- [117] J. Wang, H. Shen, L. Fan, R. Wu, B. Niu, L. T. Varghese, Y. Xuan, D. E. Leaird, X. Wang, F. Gan, A. M. Weiner, and M. Qi, "Reconfigurable radio-frequency arbitrary waveforms synthesized in a silicon photonic chip," *Nature Commun.*, vol. 6, p. 5957, Jan. 2015.
- [118] C. Taddei, L. Zhuang, M. Hoekman, A. Leinse, R. Oldenbeuving, P. van Dijk, and C. Roeloffzen, "Fully reconfigurable coupled ring resonator-based bandpass filter for microwave signal processing," in *Proc. Asia-Pacific Microwave Photonics Conf. Int. Topical Meeting Microwave Photonics*, Oct. 20–23, 2014, pp. 44–47.
- [119] B. J. Eggleton, B. Luther-Davies, and K. Richardson, "Chalcogenide photonics," *Nat. Photon.*, vol. 5, pp. 141–148, Feb. 2011.
- [120] B. J. Eggleton, T. D. Vo, R. Pant, J. Schr, M. D. Pelusi, D. Y. Choi, S. J. Madden, and B. Luther-Davies, "Photonic chip based ultrafast optical processing based on high nonlinearity dispersion engineered chalcogenide waveguides," *Laser Photon. Rev.*, vol. 6, no. 1, pp. 97–114, 2012.
- [121] K. Tan, D. A. I. Marpaung, R. Pant, F. Gao, E. Li, J. Wang, D. Y. Choi, S. Madden, B. Luther-Davies, J. Sun, and B. J. Eggleton, "Photonic-chip-based all-optical ultra-wideband pulse generation via XPM and birefringence in a chalcogenide waveguide," *Opt. Express*, vol. 21, no. 2, pp. 2003–2011, 2013.
- [122] R. Pant, A. Byrnes, C. G. Poulton, E. Li, D.-Y. Choi, S. Madden, B. Luther-Davies, and B. J. Eggleton, "Photonic-chip-based tunable slow and fast light via stimulated Brillouin scattering," *Opt. Lett.*, vol. 37, no. 5, pp. 969–971, 2012.
- [123] M. Pagani, D. Marpaung, D.-Y. Choi, S. J. Madden, B. Luther-Davies, and B. J. Eggleton, "Tunable wideband microwave photonic phase shifter using on-chip stimulated Brillouin scattering," *Opt. Express*, vol. 22, no. 23, p. 28810, 2014.
- [124] A. Byrnes, R. Pant, E. Li, D. Y. Choi, C. G. Poulton, S. Fan, S. Madden, B. Luther-Davies, and B. J. Eggleton, "Photonic chip based tunable and reconfigurable narrowband microwave photonic filter using stimulated Brillouin scattering," *Opt. Express*, vol. 20, no. 17, pp. 18836–18845, 2012.
- [125] S. Iezekiel, "Measurement of microwave behavior in optical links," *IEEE Microwave Mag.*, vol. 9, no. 3, pp. 100–120, 2008.
- [126] M. Feng, N. Holonyak, Jr., G. Walter, and R. Chan, "Room temperature continuous wave operation of a heterojunction bipolar transistor laser," *Appl. Phys. Lett.*, vol. 87, no. 13, p. 131103, 2005.
- [127] S. Iezekiel, "Microwave-photonic links based on transistor-lasers: Small-signal gain analysis," *IEEE Photon. Technol. Lett.*, vol. 26, no. 2, pp. 183–186, 2014.
- [128] D. Perez, I. Gasulla, and J. Capmany, "Microwave photonics transistor design equations," in *Proc. 9th Asia-Pacific Microwave Photonics Conf. Int. Topical Meeting IEEE Microwave Photonics*, 2014, pp. 82–85.
- [129] M. Liu, X. Yin, E. Ulin-Avila, B. Geng, T. Zentgraf, L. Ju, F. Wang, and X. Zhang, "A graphene-based broadband optical modulator," *Nature*, vol. 474, pp. 64–67, 2011.
- [130] B. Sensale-Rodriguez, R. Yan, L. Liu, D. Jena, and H. G. Xing, "Graphene for reconfigurable terahertz optoelectronics," *Proc. IEEE*, vol. 101, no. 7, pp. 1705–1716, 2013.

